

Analysis of the atmospheric distribution, sources, and sinks of oxygenated volatile organic chemicals (OVOC) based on measurements over the Pacific during TRACE-P

H. B. Singh¹, L. J. Salas¹, R. B. Chatfield¹, E. Czech¹, A. Fried², J. Walega², M. J. Evans³, B. D. Field³, D. J. Jacob³, D. Blake⁴, B. Heikes⁵, R. Talbot⁶, G. Sachse⁷, J. H. Crawford⁷, M. A. Avery⁷, S. Sandholm⁸, H. Fuelberg⁹

¹ NASA Ames Research Center, Moffett Field, CA 94035

² National Center for Atmospheric Research, Boulder, CO, 80307

³ Harvard University, Cambridge, MA 02138

⁴ University of California, Irvine, CA 92697

⁵ University of Rhode Island, RI 02882

⁶ University of New Hampshire, Durham, NH 03824

⁷ NASA Langley Research Center, Hampton, VA 23665

⁸ Georgia Institute of Technology, Atlanta, GA 30332

⁹ Florida State University, Tallahassee, FL 32306

(TRACE-P special issue II, submitted to JGR-Atmospheres, June 2003)

Abstract. Airborne measurements of a large number of oxygenated volatile organic chemicals (OVOC) were carried out in the Pacific troposphere (0.1-12 km) in Winter/Spring of 2001 (Feb. 24-April 10). Specifically these measurements included acetone (CH_3COCH_3), methylethyl ketone ($\text{CH}_3\text{COC}_2\text{H}_5$, MEK), methanol (CH_3OH), ethanol ($\text{C}_2\text{H}_5\text{OH}$), acetaldehyde (CH_3CHO), propionaldehyde ($\text{C}_2\text{H}_5\text{CHO}$), PANs ($\text{C}_n\text{H}_{2n+1}\text{COO}_2\text{NO}_2$), and organic nitrates ($\text{C}_n\text{H}_{2n+1}\text{ONO}_2$). Complementary measurements of formaldehyde (HCHO), methyl hydroperoxide (CH_3OOH), and selected tracers were also available. OVOC were abundant in the clean troposphere and were greatly enhanced in the outflow regions from Asia. Background mixing ratios were typically highest in the lower troposphere and declined towards the upper troposphere and the lowermost stratosphere. Their total abundance (ΣOVOC) was nearly twice that of nonmethane hydrocarbons ($\Sigma\text{C}_2\text{-C}_8\text{ NMHC}$). Throughout the troposphere, the OH reactivity of OVOC is comparable to that of methane and far exceeds that of NMHC. A comparison of these data with western Pacific observations collected some seven years earlier (Feb.-March, 1994) did not reveal significant differences. Mixing ratios of OVOC were strongly correlated with each other as well as with tracers of fossil and biomass/biofuel combustion. Analysis of the relative enhancement of selected OVOC with respect to CH_3Cl and CO in twelve plumes originating from fires and sampled in the free troposphere (3-11 km) is used to assess their primary and secondary emissions from biomass combustion. The composition of these plumes also indicates a large shift of reactive nitrogen into the PAN reservoir thereby limiting ozone formation. A 3-D global model, that uses state of the art chemistry and source information, is used to compare measured and simulated

mixing ratios of selected OVOC. While there is reasonable agreement in many cases, measured aldehyde concentrations are significantly larger than predicted. At their observed levels, acetaldehyde mixing ratios are shown to be an important source of HCHO (and HO_x) and PAN in the troposphere. Based on presently known chemistry, measured mixing ratios of aldehydes and PANs are mutually incompatible. We provide rough estimates of the global sources of several OVOC and conclude that collectively these are extremely large (150-500 TgC y⁻¹) but remain poorly quantified.

1. Introduction

In recent years it has become evident that significant concentrations of a large number of oxygenated organic chemicals (OVOC) are present in the global troposphere [Singh et al., 2001]. While the role of formaldehyde (HCHO) as a product of methane oxidation has been studied for over two decades, interest in other OVOC is relatively new. These chemicals are expected to play an important role in the chemistry of the atmosphere. For example, acetone can influence ozone chemistry by sequestering nitrogen oxides (NO_x) in the form of PAN and by providing HO_x free radicals in critical regions of the atmosphere [Singh et al. 1994, 1995; McKeen et al., 1997; Wennberg et al., 1998; Jeagle et al. 2001]. OVOC may also contribute to organic carbon in aerosol via cloud interactions and processes of polymerization [Li et al., 2000; Jang et al., 2002; Tabazadeh et al., 2003]. OVOC are believed to have large terrestrial sources but our quantitative knowledge about these is rudimentary [Singh et al. 1994; Guenther et al., 1995, 2000; Fall, 1999, 2003; Jacob et al., 2002; Galbally et al., 2002; Heikes et al. 2002]. Attempts to reconcile atmospheric observations with known sources have led to suggestions that oceanic sources may be quite significant although no direct evidence is presently available [de Laat et al., 2001; Singh et al., 2001, 2003; Jacob et al., 2002].

The spring 2001 TRACE-P study utilized the NASA/DC-8 flying laboratory to measure a large number of OVOC and chemical tracers in the polluted and unpolluted Pacific troposphere. An overview of the mission payload, flight profiles, and prevalent meteorological conditions has been provided by Jacob et al. [2003] and Fuelberg et al. [2003]. Here we investigate and analyze the distribution of oxygenated chemicals in the troposphere and the lowermost stratosphere, and use their relationships with select tracers along with models to assess their sources and fate.

2. Experimental

Results presented here are principally based on measurements carried out by the NASA Ames group aboard the NASA/DC-8 aircraft using the PANAK (PAN-Aldehydes-Alcohols-Ketones) instrument package. PANAK, a 3-channel gas chromatographic instrument equipped with capillary columns and multiple detectors, was used to measure oxygenated species and selected tracers. Specifically these measurements included acetone (CH₃COCH₃, propanone), methylethyl ketone (CH₃COC₂H₅, butanone, MEK), methanol (CH₃OH), ethanol (C₂H₅OH), acetaldehyde (CH₃CHO; ethanal), propionaldehyde (C₂H₅CHO, propanal), PANs, (C_nH_{2n+1}COO₂NO₂, peroxyacyl nitrates), and alkyl nitrates (C_nH_{2n+1}ONO₂). The basic instrument has been previously described and details are not repeated here [Singh et al., 2000; 2001; 2002]. Briefly, PAN, PPN, alkyl nitrates and C₂Cl₄, were separated on two GC columns equipped with electron capture detectors; while carbonyls, alcohols, and nitriles were measured on the third column in which a photo-ionization detector (PID) and a Reduction Gas Detector (RGD) were placed in series. Typically a 200 ml aliquot of air was cryogenically trapping at -140°C prior to analysis. For carbonyl/alcohol/nitrile analysis, moisture was greatly reduced by passing air through a water trap held at -40°C during sampling and 50°C between samples. Laboratory tests were performed to ensure the integrity of oxygenates during this drying process. Standard addition procedures were used for in-flight calibrations. Standard mixtures in air (or N₂) were obtained using diffusion tubes for PAN and both permeation tubes and pressurized cylinders for carbonyls, alcohols, and

alkyl nitrates. The sensitivity of detection of reactive nitrogen species was ≈ 1 ppt, while that of other oxygenates was 5-20 ppt. Overall measurement precision and accuracy are estimated to be $\pm 10\%$ and $\pm 20\%$, respectively except perhaps for $>C_1$ -aldehydes. There was indication of artifact OVOC formation under high O_3 concentrations in the stratosphere. Subsequent laboratory tests show that for the typical O_3 levels encountered in the troposphere during TRACE-P (10-100 ppb), enhancements due to this artifact were probably small (0 to 20%) and no corrections to the data have been applied. A chromatogram showing the separation and detection of alcohols and carbonyls from ambient air is shown in Figure 1. Other chemicals considered in this study include HCHO and CH_3OOH whose measurement methods have also been previously described [Fried et al., 2003; O'Sullivan et al., 2003]. In addition, a large number of non-methane hydrocarbons (NMHCs), as well as tracers of urban pollution (e. g. CO , C_2Cl_4), biomass combustion (e. g. CH_3Cl), and marine emissions (e. g. $CHBr_3$) were analyzed from pressurized canister samples [Blake et al., 1999].

3. Results and Discussion

In this study we analyze and interpret measurements of carbonyls, alcohols, and organic peroxides performed aboard the NAS/DC-8 during TRACE-P. Some of these measurements were duplicated using independent techniques and have been discussed further by Eisele et al. [2003]. In the analysis that follows, we use measurements of $>C_1$ -carbonyls and alcohol from the NASA Ames group, HCHO from the NCAR group [Fried et al., 2003], and CH_3OOH from the University of Rhode Island group [Lee et al., 1995; O'Sullivan et al., 2003]. This somewhat subjective selection took into account factors such as known shortcomings in techniques and anomalous data behavior against known tracers. To relate measurements acquired at differing frequencies, merged data files were created. In much of the analysis that follows the 5-min merged data set has been used. When appropriate, the pacific region has been divided into areas representing the western Pacific (Longitude 100-180°E) and central/eastern Pacific (Longitude 160-240°E). Unless noted otherwise, only data from the troposphere are considered. A convenient filter ($O_3 > 100$ ppb for $z > 10$ km; also $CO < 50$ ppb) was used to remove stratospheric influences. We used methyl chloride (CH_3Cl) and potassium as tracers of biomass combustion, and CO as a more generic tracer of pollution. Although CH_3Cl is known to have a diffuse oceanic and possibly biogenic source [Butler, 2000], it was possible to use it as a tracer of biomass combustion in discreet plumes downwind of terrestrial sources. Tetrachloroethylene (C_2Cl_4), a synthetic organic chemical, was mainly used as a tracer of urban pollution. When appropriate, an arbitrary "pollution filter" based on the lower two quartiles of the CO and C_2Cl_4 mixing ratios was employed to mitigate the effect of pollution. Figure 2 shows the CO mixing ratios as a function of latitude and their frequency distribution with and without this "pollution filter". This filter eliminated all major pollution influences and resulted in mean tropospheric mixing ratios of $102(\pm 20)$ ppb/ CO and $3(\pm 1)$ ppt/ C_2Cl_4 , and is assumed to represent near-background conditions.

The analysis of OVOC measurements is further facilitated by the use of the GEOS-CHEM 3-D global model. Here the troposphere is divided into 20 vertical layers and the model has a horizontal resolution of 2° latitude x 2.5° longitude. The model uses assimilated meteorology from the NASA Global Modeling and Assimilation Office, and includes an extensive representation of ozone- NO_x -VOC chemistry (80 species, 300 reactions). The model simulations were conducted for the TRACE-P period and model results were sampled along the aircraft flight tracks. More details about the GEOS-CHEM model and its applications can be found elsewhere [Bey et al. 2001; Jacob et al. 2002; Staudt et al., 2003; Heald et al., 2003]. The 3-D model simulations were available along the flight tracks for the entire TRACE-P period. An updated version of an earlier 1-D model [Chatfield et al., 1996] with detailed C_1 - C_4 hydrocarbon chemistry was also employed as an exploratory tool to study the potential role of CH_3CHO in atmospheric chemistry.

3.1. Atmospheric Distributions

3.1.1. TRACE-P measurements and 3-D model simulations

Tropospheric mixing ratios (mean, median, and σ) of important OVOC and select tracers measured in this study are presented in Table 1. Mixing ratios are shown with a 2-km vertical resolution with and without the "pollution filter" described above. A dramatic effect of the "pollution filter" can be seen in PAN whose median marine boundary layer (MBL, 0-2 km) mixing ratios declined from 165 ppt to 2 ppt (Table 1). Except in the case of CH_3OOH , mixing ratios of OVOC were elevated under polluted conditions. CH_3OOH is an exception whose mixing ratios are lower under polluted conditions (Table 1). This is to be expected as its synthesis is most efficient under low NO_x conditions, typically associated with unpolluted air [Lee et al., 2000]. Mean mixing ratios of all of the measured OVOC with the "pollution filter" are presented in Figure 3A in 1 km altitude bins. Methanol and

CH_3COCH_3 are clearly the most abundant with median concentrations of 649 ppt and 537 ppt, respectively. However, sizable concentrations of a host of other oxygenates are present. CH_3OOH mixing ratios are large in the marine boundary layer (MBL, 0-2 km) and decline rapidly in the free troposphere. In the free troposphere total alkyl nitrates (TAN, ΣRONO_2) and PPN mixing ratios are quite small and nearly 90% of the organic reactive nitrogen is contained in the form of PAN. Although MEK has been previously measured in urban and rural environments [Grosjean et al., 1982; Snider and Dawson, 1985; Fehsenfeld et al., 1992; Golden et al., 1995; Solberg et al., 1996; Riemer et al., 1998], these are its first measurements in the remote troposphere. Its median abundance of 20 ppt in the clean troposphere is a small fraction of CH_3COCH_3 (537 ppt).

An unusual finding from Figure 3A is that large mixing ratios of CH_3CHO , exceeding those of HCHO , are found to be present. We also report the first tropospheric profile of $\text{C}_2\text{H}_5\text{CHO}$. Measurements of CH_3CHO and $\text{C}_2\text{H}_5\text{CHO}$ in the free troposphere from other regions vary from sparse to nonexistent. However, CH_3CHO data from the MBL have been published from a number of locations utilizing a variety of measurement techniques. Mean CH_3CHO mixing ratios of 100-400 ppt in the MBL have been reported from the northern and southern Pacific [Singh et al., 1995; 2001], the Atlantic [Zhou and Mopper, 1993; Arlander et al., 1995; Tanner et al., 1996], and the Indian Ocean [Wisthaler et al., 2002]. Not all the methods used are equally reliable and the wet chemical derivative methods are often prone to interferences. Wisthaler et al. [2002], using a new mass spectrometric technique, report MBL mixing ratios of 212 ± 29 ppt and 178 ± 30 ppt from the northern (0-20 °N) and southern (0-15 °S) Indian Ocean, respectively under the cleanest conditions. This can be compared with the pollution-filtered MBL (0-2 km) mixing ratios of 204 ± 40 ppt measured in this study over the NH-Pacific (Table 1). The ensemble of observations supports the view that substantial CH_3CHO concentrations are present throughout the global troposphere. No comparable measurements of $\text{C}_2\text{H}_5\text{CHO}$ are available. As we shall see later, $\text{C}_2\text{H}_5\text{CHO}$ and CH_3CHO behave very similarly and it is likely that $\text{C}_2\text{H}_5\text{CHO}$ is also globally ubiquitous albeit at lower mixing ratios (MBL: 68 ± 24 ppt).

Collectively, these OVOC are nearly twice as abundant as all C_2 - C_8 hydrocarbons combined (Figure 3B). Based on these measurements and the kinetic data available from Atkinson et al. [2002] and Sander et al. [2002], we calculate that the OH oxidation rate of OVOC ($\Sigma \text{C}_{\text{ovoci}} \times k_{\text{OHi}}$) in the troposphere is comparable to that of methane ($\Sigma \text{C}_{\text{CH}_4} \times k_{\text{OHi}}$) and some five times larger than that of NMHC ($\Sigma \text{C}_{\text{NMHCi}} \times k_{\text{OHi}}$). Compared to NMHC, mixing ratios of OVOC declined rather slowly towards the upper troposphere (UT). In addition, strong latitudinal gradients were present. Figure 4 shows the latitudinal distributions of selected OVOC in the UT (8-12 km) for the data set with the “pollution filter”. A north to south gradient in virtually all cases, except HCHO , can be seen. CH_3OOH distribution was somewhat more complex and showed a minimum at around 25 °N that coincided with the NO_x maxima in a manner consistent with expectations (Lee et al., 2000). Lack of any latitudinal trend in HCHO is in part due to measurements close to the limit of detection (~ 30 ppt at 2σ for 5-minute averages) and in part due to the homogeneity of the sources and sinks in the UT. This north-south latitudinal behavior for these gases is mainly dictated by the presence of more efficient removal (higher OH and hv) at the lower latitudes and is broadly captured by the GEOS-CHEM model [Field et al., 2003].

During TRACE-P, air masses representing the lowermost stratosphere ($\text{O}_3 < 700$ ppb) were occasionally sampled. Figure 5 presents these data for a select set of chemicals. A rapid decline in the concentrations of CO, PAN, CH_3COCH_3 , and CH_3OH as a function of O_3 is evident. Ethanol was below its detection limit here, and extremely high O_3 concentrations precluded reliable measurements of CH_3CHO and CH_3OOH . A relatively low level of OVOC is present in the lower stratosphere. We further note that our measurement methods have not been tested for stratospheric conditions. These results are in general agreement with previous findings [Arnold et al. 1997; Singh et al., 2000].

Figure 6 shows the vertical structure of a selected group of OVOC that were also simulated by the GEOS-CHEM model. The model simulations are along the flight tracks and are segregated into subsets with “pollution filter” (bottom panels) and without it (top panels). This model is successful in simulating mean structures of chemicals with large primary (e. g. CH_3COCH_3) as well as secondary sources arising from NMHC/ NO_x (e. g. PAN) and CH_4/NO_x (e. g. CH_3OOH) chemistry. It is not our intention to imply that the GEOS-CHEM simulations are accurate under all conditions, but rather that it is possible to capture the mean structures. More detailed analysis by Field et al., [2003] shows that the model can only partially explain the observed latitudinal structures. In many cases, poor knowledge of sources, as well as sinks, does not allow accurate simulations. For example, the model significantly over predicts CH_3COCH_3 in the MBL. In large part this is due to the inclusion of a rather large oceanic source (14 Tg y^{-1}) inferred by Jacob et al. [2002] via inverse modeling. Trace-P observations imply that the oceanic CH_3COCH_3 emissions may be much smaller than assumed. Singh et al. [2003] argue that the Trace-P data are consistent with an oceanic sink of acetone.

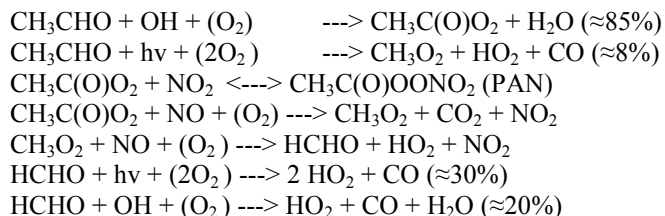
In Figure 7 we plot the observed and modeled altitude profile for CH_3OH and the $\text{CH}_3\text{OH}/\text{CH}_3\text{COCH}_3$ ratio for the filtered data set. It is expected that ratios of these chemicals would help to normalize some of the dynamical

inaccuracies in the model. A significant divergence in the measured and modeled mixing ratios can be seen. One could infer the presence of unknown CH_3OH sinks in the free troposphere not presently simulated and/or the presence of incorrect CH_3OH sources in the model. Except for HCHO , all of the OVOC considered in this study are quite insoluble [Sander, 1999] and rainout/washout processes are expected to be unimportant. Yokelson et al [2003] studied one cloud system over fires in South Africa and found complete depletion of CH_3OH within a 10-min period. Tabazadeh et al. [2003] have further investigated these observations and conclude that heterogeneous reactions on cloud droplets may be responsible for this loss. Gas phase and liquid phase reactions with OH , Cl , HCl , NO_2 cannot explain the observed rapid disappearance of methanol. To test the hypothesis of methanol losses in clouds, TRACE-P data were segregated into in-cloud and clear air categories [Crawford et al., 2003]. A comparison of the mixing ratios in and out of clouds is shown in Figure 8 directly and when normalized to CO . There is clear evidence of higher pollutant levels within clouds due to convective uplifting. The median in-cloud $\text{CH}_3\text{OH}/\text{CO}$ ratio of 6.7 is somewhat lower than the 7.2 found in clear air but this difference is statistically insignificant. No conclusive evidence for CH_3OH loss due to cloud processes could be ascertained from TRACE-P measurements. Tabazadeh et al. [2003] point out that insufficient residence time within clouds may have been an important factor. Other potential heterogeneous loss involving reaction with acidic aerosol can also be discounted [Iraci et al., 2002]. The potential role of CH_3OH in heterogeneous chemistry is presently poorly understood and needs further investigation.

Figure 9, shows a comparison of observed and GEOS-CHEM model simulated mixing ratio of several aldehydes measured during Trace-P. As has been noted before [Singh et al., 2001], the simulated concentrations of CH_3CHO and $\text{C}_2\text{H}_5\text{CHO}$ are much smaller than observed. At the same time the model provides a reasonable description of HCHO which is principally a product of methane oxidation. Although comparably high CH_3CHO mixing ratios have also been reported from the Atlantic and the Indian Ocean regions using completely independent measurement techniques [Arlander and Brunking, 1995; Wisthaler et al., 2002], we are unable to fully reconcile these observations with current knowledge of atmospheric chemistry. Model simulations show that the observed CH_3CHO and PAN concentrations are mutually incompatible [Staudt et al., 2003]. Observed $\text{C}_2\text{H}_5\text{CHO}/\text{CH}_3\text{CHO}$ ratios would suggest PPN/PAN ratios that are larger than actually measured. In a subsequent section we speculate on the magnitude and nature of the source(s) required to maintain the observed aldehyde levels.

3.1.2 Acetaldehyde and its potential role in HO_x formation

The gas phase reaction sequence of CH_3CHO is thought to be well known. It is mainly oxidized by reaction with OH radicals and to a lesser degree decomposed by photolysis. These reaction rates and absorption crosssections have been extensively measured [Atkinson et al, 2002; Sander et al., 2002; Martinez et al., 1992; Finlayson-Pitts and Pitts, 1999]. Under relatively high NO conditions, above 50 ppt, the reaction of acetaldehydes leads rapidly to HCHO and HO_x . Müller and Brasseur [1999] estimate that the net HO_x yield from CH_3CHO in the UT is 0.3-0.5. Rapid injection of CH_3CHO from the lower troposphere to the UT via deep convection will further influence UT chemistry. Under very low NO concentrations competing reactions become important and other products such as hydroperoxides, alcohols, acids and hydroxy-acids are favored.



We further investigated the role of CH_3CHO on HCHO (and HO_x) formation in the troposphere using the present observations and a 1-D model with updated chemistry [Chatfield et al., 1996]. Results from a number of simulations are summarized in Figure 10. The solid red line shows the steady state concentration of HCHO consistent with a simulation that maintains the CH_3CHO and CH_3COCH_3 at observed levels. The dotted red line shows HCHO calculated for a situation in which only acetone is maintained at observed values, but acetaldehyde produced only from secondary hydrocarbon reactions. In both cases, the hydroperoxides are calculated to be in a self-consistent steady state. As is evident from the difference between solid and dashed red lines in Figure 10, observed CH_3CHO can contribute an extra 25 ppt or more HCHO throughout most of the troposphere. This HCHO is a direct source of additional HO_x in the troposphere. Consistent with the results of Staudt et al. [2003], the observed CH_3CHO mixing ratios produced far greater PAN than was measured (Figure 10). Propionaldehyde is

expected to behave in a similar manner, producing a small amount CH_3CHO , HCHO , HO_x and PPN. These large mixing ratios of CH_3CHO , if proven correct, provide a major perturbation to our present understanding of tropospheric chemistry.

3.1.3. Comparison of TRACE-P and PEM-West B Observations

PEM-West B was an exploratory mission performed over the western Pacific in Winter/Spring of 1994 (Feb.-March). It used the NASA DC-8 aircraft and measured many of the same constituents. It is instructive to compare these two data sets collected 7 years apart. During PEM-West B oxygenated species could only be measured in the free troposphere due to difficulties associated with water interference. Although these difficulties were overcome in TRACE-P, comparisons here are restricted to altitudes >3 km. The sampling density in these two experiments was quite different and certain regions were not sampled in PEM-West B (e. g. Yellow Sea). Therefore the purpose of the comparison that follows is primarily to assess gross differences in composition and emission patterns.

A comparison of the mean/median mixing ratios of CO , O_3 , and NO_x under “clean” and “polluted” conditions is presented in Figure 11 for mid-latitudes ($25\text{--}45^\circ\text{N}$) and tropical/subtropical latitudes ($10\text{--}25^\circ\text{N}$). We note that such comparisons may be least meaningful for short-lived species with inhomogeneous sources such as NO_x ($\tau = 1\text{--}4$ days). It is evident that CO concentrations were essentially unchanged in the background as well as the polluted troposphere over this 7-year period at both mid- and tropical/subtropical latitudes. Atmospheric mixing ratios of several select species measured in TRACE-P and PEM-West B are also plotted as a function of CO in Figure 12. There are no obvious large differences in these two data sets. The similarity was as true of tracers of biomass (CH_3Cl) and fossil fuel (C_6H_6) combustion, as of complex photochemical species such as PAN. Although concentrations of CH_3COCH_3 and CH_3OH are slightly higher in TRACE-P, these differences are small and within the uncertainties of measurements.

As can be seen from Figure 11, mean/median O_3 mixing ratios during these two experiments were nearly equal at subtropical latitudes under all conditions. At mid-latitudes the background atmosphere ($\text{CO} < 125$ ppb) also showed little discernable change. However, in the polluted air masses O_3 during TRACE-P were larger by about 20 ppb. This excess is also evident in the outflow regions in Figure 12. An analysis based on NMHC ratios, ruled out large differences in air mass ages. A logical answer could be that NO_x concentrations in the outflow regions were higher during TRACE-P compared with PEM-West B. Economic indicators show that there has been a greater use of fossil fuels in Asia during this period. However, such an answer is not conclusive as higher NO_x levels did not appear to result in high O_3 at subtropical latitudes. Davis et al. [2003] have investigated these ozone changes in detail and concluded that the 14-day delay between these two missions altered the ozone chemistry sufficiently to be an important factor in the net O_3 formation at mid-latitudes. These tendencies were not affected at subtropical latitudes. On the whole, comparison of data from TRACE-P and PEM-West B, separated by 7-years, failed to reveal any dramatic changes in the composition of the Pacific troposphere.

3.2. Tracer Relationships and Source Characteristics

3.2.1 Atmospheric relationships

Despite a high degree of variability, mixing ratios of OVOC were correlated suggesting a commonality of sources. Figure 13 shows this linear relationship with CO and CH_3Cl in the free troposphere (3-12 km) over the entire Pacific for a selected aldehyde, ketone, and alcohol. These relationships were maintained even in the UT (8-12 km) region of the atmosphere. Figure 14 further shows that the mixing ratios of OVOC are internally related. Thus CH_3COCH_3 behaved in a manner similar to CH_3OH and MEK. The strongest association is seen between CH_3CHO and $\text{C}_2\text{H}_5\text{CHO}$. In their entirety, these relationships provide broad support for the view that OVOC have common sources, and their atmospheric burden is strongly influenced by pollution events originating from fossil fuel and biomass combustion.

3.2.2 Plume composition and biomass burning source estimates

During TRACE-P several plumes originating from biomass combustion were sampled in the free troposphere (3-11 km). Five-day back trajectory analysis [Fuelberg et al., 2003], indicated that the free tropospheric plumes generally originated over regions of southern China, southeast Asia, and northern Africa. Satellite observations showed that fires were prevalent in these regions. It is common knowledge that air masses from biomass burning (BB) regions are easily advected into the free troposphere. All of the relevant tracers of biomass combustion (e. g. HCN , CH_3CN , CO , CH_3Cl , and K) were significantly elevated in these plumes. Based on these considerations, 12 plumes were studied whose origin was indicated to be from biomass combustion. As a first step we looked at the molar enhancement ratios (ERs) of selected chemicals relative to CH_3Cl and CO in these 12 plumes. These data are summarized in Table 2. Because of its BB source specificity and lack of fossil fuel source, we first use ERs with

respect to CH_3Cl to assess BB sources of selected OVOC. While somewhat less robust, because of the possibility of fossil sources, we also investigate these with respect to CO. As we shall see, there is evidence that the contribution of non-BB CO in these FT plumes was quite small. We also note that most of the ERs reported in the literature from previous studies are given with respect to CO. For purposes of scaling, we adopt a global BB CH_3Cl source of 0.9 Tg y^{-1} and a corresponding CO source of 600 Tg y^{-1} based on recent evaluations [Lobert et al., 1999; Andreae and Merlet, 2001; Duncan et al., 2003; Yevich and Logan, 2003].

For extremely short-lived species (e. g. aldehydes), ER's may have no unique value and cannot be interpreted without a detailed chemical model. Acetone and CH_3OH , however, are sufficiently long lived in the FT ($\tau \approx 15$ days) and the sampled plumes are sufficiently fresh (<5 days), that the changes (mostly reductions) in ER's due to chemical losses during transport should be small ($<25\%$). The corresponding loss for MEK and $\text{C}_2\text{H}_5\text{OH}$ is nearly twice as large. Photochemical synthesis however, can provide a secondary source during transport and is thought to be a main reason for the large spread in acetone-ER's summarized by Reiner et al. [2001] and Jost et al. [2002]. Secondary formation in BB plumes is probably far less important for alcohols.

In Table 2 we determine mean ER^{CO} (ppt/ppb) of 7.5 ± 1.1 and 16.3 ± 2.0 for CH_3COCH_3 and CH_3OH , respectively. These are two chemicals for which previous data, largely based on controlled fires, are available. Acetone- ER^{CO} is in good agreement with our previous measurements from African fires (8 ± 2) [Mauzurall et al., 1998] but somewhat higher than those reported by Holzinger et al. [1999] (5.4 ± 2.7) from simulated laboratory fires. Similarly, mean methanol- ER^{CO} is in good agreement with values of 17.1 ± 7.6 [Yokelson et al., 1999], 13.6 ± 3.9 [Yokelson et al., 2003], and 12 ± 1 [Wisthaler et al., 2002] reported in several independent campaigns from widely separated regions. No published data for MEK or ethanol ER's could be uncovered. Although we suspect that short-lived species such as CH_3CHO may have no unique ER, the CH_3CHO ER^{CO} (ppt/ppb) of 1.4 ± 0.8 can be compared with 3.5 ± 1.9 measured by Hurst et al. [1994] in Australian fires. ER's with respect to CH_3Cl have not been previously reported.

Rough BB source estimates can be obtained by scaling Table 2 ER's to the BB sources of CO (600 Tg y^{-1}) and CH_3Cl (0.9 Tg y^{-1}). This assumes that 12 plumes sampled during TRACE-P provide a representative sample. Given the great paucity of available data, this assumption is at least a good first starting point. Table 2 summarizes these source estimates calculated for selected oxygenated species. We note that values derived from ER^{CO} and $\text{ER}^{\text{CH}_3\text{Cl}}$ are very nearly the same. This supports the assumption that CO contamination from fossil sources was minimal in these plumes. A global BB source of 9 Tg y^{-1} for CH_3COCH_3 and 11 Tg y^{-1} for CH_3OH is calculated. The CH_3OH estimate of 11 Tg y^{-1} is in good agreement with many of the recent estimates summarized in Table 3. The estimated source of CH_3COCH_3 is substantially larger than the Andreae and Merlet [2001] recommendation of 3.3 Tg y^{-1} . As stated above, some synthesis of CH_3COCH_3 can occur from BB precursors during transport. In a recent study, Jost et al. [2003] use a detailed model to conclude that they are unable to simulate the enhancement of CH_3COCH_3 within a BB plume possibly due the presence of unknown precursors or reaction mechanisms. Therefore we recommend that for global model simulations the use of the larger source term (9 Tg y^{-1}), that includes primary and a significant fraction of the secondary source, is more appropriate. After correcting ER's for the $\approx 50\%$ reduction during transit, a smaller BB source of about 2 Tg y^{-1} each for MEK and $\text{C}_2\text{H}_5\text{OH}$ can be estimated (Table 2 and 3). There are no published values available for comparison.

The mean ozone- ER^{CO} of $0.3 (\pm 0.2)$ ppb/ppb measured during TRACE-P (Table 2) is similar to that obtained for "recent plumes" originating from African fires [Mauzurall et al., 1998]. We note that in some of the aged plumes there was no measurable ozone enhancement. This somewhat low ozone- ER^{CO} can be attributed to the fact that much of the reactive nitrogen appears to shift into the PAN reservoir and is not readily available for further O_3 synthesis. On average some 65% of the reactive nitrogen was in the form of PAN, 22% as HNO_3 , and 13% as NO_x (Table 2). When aged plumes were selected, some 85% of reactive nitrogen was found to be in the PAN reservoir (HNO_3 :8%; NO_x :6%). As has been suggested previously [Jacob et al., 1996; Mazurall et al., 1998], O_3 production in fire plumes is controlled by the availability of NO_x from the PAN reservoir and is thus considerably impeded.

Several episodes of pollution outflow from eastern Asia were also sampled in the marine boundary layer (MBL). These ER's are also summarized in Table 2 based on the sampling of 9 such episodes (0-1 km). The quantitative interpretation of these ER's is difficult due to the extreme complexity of urban sources in Asia. However, since CH_3Cl is not a product of fossil fuel combustion, one can make some qualitative observations. It appears that biofuels and coal, common fuels in eastern Asia, yield somewhat less CH_3COCH_3 and CH_3OH compared to active fires. In the case of CH_3COCH_3 a shorter residence time providing insufficient time for synthesis is a factor. It can also be inferred that substantial additional urban sources of MEK are present. This is not a surprise as significant quantities of MEK are commercially used in solvent applications and it can also be relatively rapidly (hours) synthesized from the oxidation of fossil fuel generated hydrocarbons such as n-butane.

3.2.3. Global sources

Due to the complexity of sources and lack of observational data, our quantitative knowledge of OVOC emissions is quite incomplete. Emissions have been estimated by extrapolating limited laboratory and field studies or derived from atmospheric measurements using a variety of inversion methods. In most cases a combination of these approaches have been used. Biogenic emissions are significant in nearly all cases but remain poorly quantified. Biological pathways involved in the formation of OVOC in plant matter have been recently reviewed by Fall [2003]. Here we assess the current state of knowledge of select OVOC emissions and further interpret these in light of present measurements. Given the great paucity of available data, many assumptions and extrapolations are necessary and are noted. Estimates of the global sources of OVOC are presented in Table 4. These are intended to show uncertainties in our present knowledge in some cases and provide an initial estimate in others. While uncertainties abound, a large global OVOC source of some 300 (150-500) TgC y⁻¹ appears to be present.

Acetone: Of the many OVOC present in the atmosphere, CH₃COCH₃ is one of the most abundant and has been studied most extensively. Its first global inventory was presented in the early 90's and subsequently revised [Singh et al., 1994; 2000]. More recently, Jacob et al. [2002] have further investigated the budget of CH₃COCH₃ by reviewing existing information and by using inverse modeling techniques from which additional source information is inferred. In Table 4 we provide global source estimates of CH₃COCH₃ obtained in these two studies. The Jacob et al. [2002] study finds that a global CH₃COCH₃ source of 95 Tg y⁻¹ fits the observational data better than the 56 Tg y⁻¹ estimated by Singh et al. [2000] using inventory approaches.

Jacob et al. [2002] recommend a primary biogenic source of 33 Tg y⁻¹, nearly twice as large as Singh et al. [2000]. Recent plant emission and flux data suggest even larger primary biogenic emissions [Schade and Goldstein, 2001; Karl et al, 2002; Villanueva-Fierro et al., 2003]. Potter et al. [2003] use foliar emission and satellite derived Leaf Area Index data to obtain a global acetone biogenic source of 50-170 Tg y⁻¹. A biogenic source of 50 (25-50) Tg y⁻¹ is consistent with these data and is recommended (Table 4). Based on this study, we also find that a BB source that is nearly twice as large (9 Tg y⁻¹) is more appropriate (Table 3). This larger source includes both primary and secondary sources from BB emissions whose mechanisms are not well known [Jost et al., 2003]. Both the magnitude and the sign of the oceanic flux of CH₃COCH₃ are uncertain. Using a variety of inverse modeling methods a net oceanic source of 10-15 Tg y⁻¹ has been suggested [de Laat et al. 2001; Jacob et al. 2002]. Singh et al. [2003] use the gradient at the top of the MBL (Table 1) and an air-sea exchange models to conclude that TRACE-P observations are more compatible with an oceanic sink of 14 Tg y⁻¹. No seawater measurements are presently available to directly support the role of oceans as a source or a sink of acetone. We use these data to provide a revised source inventory of CH₃COCH₃ in Table 4 while retaining the 95 Tg y⁻¹ global source recommended by Jacob et al. [2002].

In subsequent discussion we will estimate the global source of OVOC by normalizing to this CH₃COCH₃ source (Equation 1).

$$[S]_{\text{OVOC}} (\text{Tg y}^{-1}) = (95) \times (C_{\text{OVOC}} \times M_{\text{OVOC}} \times \tau_{\text{acetone}}) / (C_{\text{acetone}} \times M_{\text{acetone}} \times \tau_{\text{OVOC}}) \quad (1)$$

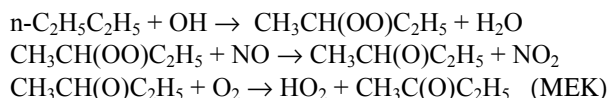
Where S, C, M, and τ are symbols used to represent emissions, mixing ratios, molecular weights, and mean lifetimes, respectively. A mean CH₃COCH₃ lifetime of 16 days and median mixing ratios for the filtered data set (Table 1) have been used in subsequent calculations. Equation 1 is approximate and its use is warranted only when no previous information is available or to assess large scale inconsistencies in source estimates from different studies.

Methanol: A first global budget of the CH₃OH was presented by Singh et al. [2000]. More recently, methanol budget has been reviewed and further investigated by Galbally et al. [2002] and Heikes et al. [2002]. It is evident from Table 4 that large uncertainties in its sources (and implied sinks) are currently present and the estimated source can range from 75-490 Tg y⁻¹. The largest disagreement is due to the widely differing estimates of its biogenic emissions (35-280 Tg y⁻¹). The Galbally et al. [2002] global source estimate of 149 Tg y⁻¹ is based on a mechanistic model of plant emissions. This estimate is comparable to the 122 Tg y⁻¹ deduced by Singh et al. [2000] using inventory methods. Using a mean atmospheric lifetime of 9 days [Heikes et al. 2002] and present measurements (Table 1), we calculate a global CH₃OH source of 110 Tg y⁻¹ from equation 1. Table 4 also shows the inventory used in the current version of the GEOS-CHEM model [Field et al., 2003]. We note that the 11 Tg y⁻¹ BB source determined in this study (Table 3) is in good agreement with previous estimates (Tables 3 and 4). As is evident from Table 1, the observed median mixing ratios of CH₃OH in the MBL (0-2 km) are lower than in the free troposphere (2-4 km) by about 200 ppt (Table 1). Singh et al. [2003] use this fact and an air-sea exchange model to conclude that oceans are near equilibrium and provide a small net sink of CH₃OH. Once again, no observational

data are presently available to support the role of oceans as a source or a sink of methanol. Emissions of CH₃OH are both large and uncertain and much further work is needed to accurately quantify these.

Methylethyl ketone (MEK): Little is known about its sources and no quantitative emissions inventory has been previously presented. Using its measured OH rate constants ($1.3 \times 10^{-12} \text{ e}^{-25/T} \text{ molec.}^{-1} \text{ cm}^3 \text{ s}^{-1}$) and its photolysis rates [Atkinson et al., 2002; Martinez et al. 1992], we determine a mean atmospheric lifetime of about 7 days. As a first estimate, a global source of about 11 Tg y⁻¹ can be calculated from equation 1. MEK is a commonly used industrial solvent and its emissions are well documented in the Toxics Release Inventory compiled by US EPA (<http://www.epa.gov/tri>). Based on these data we conclude that the direct anthropogenic emissions are insignificant as a global source (<0.1 Tg y⁻¹). MEK was also observed as an emission from decaying plant matter [Warneke et al., 1999] and has been identified as a significant biogenic emission product from a variety of plants and grasses [Isidorof et al., 1985; Kirstine et al., 1998, De Gouw et al., 1999]. Kirstine et al. [1998] report that MEK formed nearly 50% of the organic emissions from clover. The available data presently do not allow a quantitative estimation of MEK biogenic sources. In Table 4 we arbitrarily assign (by difference) $\approx 6 \text{ Tg y}^{-1}$ source to this category. Based on presently available information, an MEK source of this magnitude is quite feasible.

MEK is a unique product of the oxidation of n-butane whose global emissions are 1-2 Tg y⁻¹ [Singh and Zimmerman, 1992]. Nearly 80% of n-butane is oxidized in a manner that can produce MEK.



In addition, many alkenes (cis-2-butene/pentene, 2-methyl-1-butene etc.) also produce MEK upon reaction with O₃ and OH. Unlike the case of CH₃COCH₃, no mechanistic pathways presently appear feasible for MEK formation from the oxidation of known biogenic hydrocarbons such as isoprene, α/β pinene, and methyl butenol. We calculate that an MEK source of 2-3 Tg y⁻¹ could result from C₄-C₆ hydrocarbon oxidation with n-butane as the dominant contributor. A first estimate of the BB source of MEK (2 Tg y⁻¹) is calculated in Table 3. We expect MEK to behave like acetone with insignificant oceanic sources. These estimates are summarized in Table 4 to provide a first estimate of the global inventory of MEK.

Ethanol: Ethanol finds many applications in the commercial/industrial world. It is a commonly used solvent and is an intermediate in the manufacture of many chemicals. It is also an increasingly popular fuel and fuel additive [Nguyen et al., 2001]. Ethanol has an atmospheric lifetime of about 3.5 days and its global mixing ratios are quite small [Table 1; Singh et al., 1995]. We use equation 1 to calculate a global source of about 12 Tg y⁻¹. Its commercial/industrial/social/fuel releases and as a by product in wood product and organic chemical industry are estimated to be 1-2 Tg y⁻¹. Ethanol can also be generated as a secondary product from the oxidation of any hydrocarbon that can generate a C₂H₅O₂ radical [$2\text{C}_2\text{H}_5\text{O}_2 \rightarrow \text{C}_2\text{H}_5\text{OH} + \text{CH}_3\text{CHO} + \text{O}_2$] with ethane as the leading candidate. We use a simple photochemical model to estimate a $\approx 1 \text{ Tg y}^{-1}$ source from ethane oxidation. Ethanol has been observed as a direct emission from many plant species and high concentrations and large emission rates have been measured in many forested ecosystems and grass land areas [Kimmerer and MacDonald, 1987; Kelse et al., 1996; Lamanna and Goldstein, 1999; Schade and Goldstein, 2001; 2002; Kirstine et al., 1998; Fukui and Doskey, 1998; Karl et al., 2003]. An emission rate of some $2.9 \mu\text{g g}^{-1} \text{ dw h}^{-1}$ (30°C) was measured by Schade and Goldstein [2001] from a Ponderosa pine canopy in Blogett Forest in California. Ethanol can also be produced in plant roots by anaerobic fermentation and may metabolize to CH₃CHO and acetic acid in plant leaves prior to emission [Kreuzwieser et al., 2001]. Its metabolic pathways are well understood and in aerobic environments it can also be formed by the decomposition of CH₃CHO in plant tissues [Fall, 2003]. Its BB source is estimated to be about 2 Tg y⁻¹ [Table 3]. In Table 4 we provide a rough first analysis of its sources with the largest fraction (6 Tg y⁻¹) attributed to biogenic emissions.

Acetaldehyde: On a global scale very little is known about the sources of CH₃CHO and no global inventory is presently available. In Table 4 we provide a first, albeit highly uncertain, source inventory of CH₃CHO. From available measurements around the globe in the MBL and limited free tropospheric measurements from the Pacific, it is reasonable to assume that CH₃CHO is globally ubiquitous and its mixing ratios are substantial [Zhou and Mopper, 1993; Singh et al., 1995, 2001; Arlander et al, 1995; Tanner et al, 1996; Wisthaler et al., 2002]. As a starting point we use equation 1 to estimate its global sources. Given its very short lifetime of about 1 day and its measured atmospheric abundance (Table 1), we deduce that a total source of $\approx 220 \text{ Tg y}^{-1}$ is required and some of this must be in the free troposphere.

In a number of tail pipe emission tests [e. g. Sigsby et al., 1987], approximately 0.5% of the carbon is found to be emitted as CH_3CHO . The use of oxygenated fuels, particularly $\text{C}_2\text{H}_5\text{OH}$, results in increased tail pipe emissions of CH_3CHO . Direct emissions of CH_3CHO by industry are negligible small ($<0.1 \text{ Tg y}^{-1}$). We estimate that in total these anthropogenic emissions are $<1 \text{ Tg y}^{-1}$. Large biogenic emissions are known to occur and indeed high concentrations of CH_3CHO have been measured in many rural/forested environments [Isidorof et al., 1985; Shepson et al., 1991; Fehsenfeld et al., 1992; Goldan et al., 1995; Solberg et al., 1996; Riemer et al., 1998; Kirstine et al., 1998; Schade and Goldstein, 2001]. Direct measurements from pine and oak species show that some 0.027-0.049% of net carbon assimilated is released in the form of CH_3CHO [Kesselmeier et al., 1997]. Scaling it by the global Net Primary Productivity of $5 \times 10^4 \text{ TgC y}^{-1}$ a biogenic source of 25-45 Tg y^{-1} is feasible. These investigators also measure a direct daytime average CH_3CHO release rate of $0.83 \mu\text{g g}^{-1} \text{ dw h}^{-1}$ at 30°C . Schade and Goldstein [2001] determine mean CH_3CHO fluxes in a Ponderosa pine forest in California of $0.20 \mu\text{gC m}^{-2} \text{ dw h}^{-1}$ or $0.86 \mu\text{g g}^{-1} \text{ dw h}^{-1}$ at 30°C . Since fluxes are often reported in area units, a constant foliar density of 425 g dw m^{-2} , a typical value for Blodgett forest, has been used to obtain the corresponding mass units. They also find that nighttime emissions are extremely small ($\approx 10\%$ of daytime). Other studies summarized by Villanueva-Fierro et al. [2003] report mean rates of $0.3\text{--}1.2 \mu\text{g g}^{-1} \text{ dw h}^{-1}$ from a variety of plant species. The major exception is the study of Karl et al. [2002] who use a new technique to measure emission rates of $0.94 \mu\text{g g}^{-1} \text{ dw h}^{-1}$ at only 15°C from a site (Niwot Ridge) in Colorado. Assuming a median value of 0.7 ($0.2\text{--}1.2$) $\mu\text{g g}^{-1} \text{ dw h}^{-1}$ at 30°C only during day light hours, and a recent version of the Guenther et al. [1995] model, a CH_3CHO source estimate of 45 ($13\text{--}77$) Tg y^{-1} can be estimated. While highly uncertain, we use a reasonable central value of ≈ 35 ($20\text{--}50$) Tg y^{-1} .

Nearly all $>\text{C}_1$ -alkanes (ethane, propane, n-butane) and $>\text{C}_2$ -alkenes (propene, 2-butene) form CH_3CHO as an intermediate in their oxidation process [Finlayson-Pitts and Pitts, 1999; Warneck, 1999]. In many cases (e. g. ethane, propene) the yield of CH_3CHO is $>50\%$. In the global atmosphere the largest source must come from ethane $\{\text{C}_2\text{H}_6 + \text{OH} \rightarrow \text{C}_2\text{H}_5\text{O}_2 (+\text{NO}) \rightarrow \text{C}_2\text{H}_5\text{O} \rightarrow \text{CH}_3\text{CHO}\}$ and propene oxidation which are emitted at a rate of $15\text{--}20 \text{ Tg y}^{-1}$ and $7\text{--}12 \text{ Tg y}^{-1}$, respectively [Singh and Zimmerman, 1992]. Using a simple chemical scheme of alkane/alkene chemistry we estimate CH_3CHO source from NMHC oxidation to be ≈ 35 ($20\text{--}50$) Tg y^{-1} . BB emissions of CH_3CHO have been measured with Holzinger et al. [1999] reporting a source of 11 Tg y^{-1} and Andreae and Merlet [2001] recommending only 4 Tg y^{-1} . Based on a number of assumptions, Singh et al. [2003] estimate a global CH_3CHO oceanic source of 125 Tg y^{-1} . We note that the source inventory prescribed in Table 4, in and of itself may not be enough to explain its atmospheric budget and distribution of CH_3CHO . These estimates are also strongly dependent on the reliability of atmospheric measurements.

Propionaldehyde: Mixing ratios of $\text{C}_2\text{H}_5\text{CHO}$ are about one third of CH_3CHO and the two are highly correlated (Figure 14). There are no independent atmospheric measurements available to confirm that $\text{C}_2\text{H}_5\text{CHO}$ is indeed ubiquitous in the global troposphere. However, we use its tight correlation with CH_3CHO to suggest that it is distributed much like CH_3CHO . The lifetime of $\text{C}_2\text{H}_5\text{CHO}$, based on reaction with OH [Atkinson et al., 2002] and photolysis [Martinez et al., 1992], is also comparable to that of CH_3CHO (≈ 1 day). From these one could infer a global $\text{C}_2\text{H}_5\text{CHO}$ source of $\approx 105 \text{ Tg y}^{-1}$. Propionaldehyde is formed via photochemical oxidation of many $>\text{C}_3$ NMHCs and has been observed as a significant emission from plant matter [Villanueva-Fierro et al., 2003]. It has also been detected in seawater with substantial concentrations in the surface microlayers [Zhou and Mopper, 1997]. Singh et al. [2003] assume that the differential in the MBL between the measured and modeled mixing ratios in Figure 9 is due to the oceanic source. Based on this assumption, they estimate that an oceanic source of some 45 Tg y^{-1} must exist. Much more comprehensive atmospheric, oceanic, and emission data are required prior to any reliable source inferences.

4. Conclusions

In recent years it has become clear that large concentrations of OVOC are present in the global troposphere and they play an important role in atmospheric chemistry. Their oxidation rate is comparable to that of methane and much larger than non-methane hydrocarbons. A large ($150\text{--}500 \text{ Tg C yr}^{-1}$) carbon flux moves through the atmosphere in the form of oxygenated species. Their sources and sinks are presently highly uncertain. Biogenic emissions are nearly always significant but remain poorly quantified. The role of oceans as sources and sinks for these chemicals is largely unexplored. In many cases, measured concentrations are incompatible with our present knowledge of atmospheric chemistry. There is preliminary evidence for OVOC involvement in heterogeneous processes. The possibility that atmospheric measurement may suffer from unknown difficulties can not be ruled out. Much future work is necessary before the budgets and chemistry of this group of chemicals can be placed on a reliable quantitative footing.

Acknowledgments: This research was funded by the NASA Global Tropospheric Experiment. Harvard investigators acknowledge support from the NSF Atmospheric Chemistry Program. We thank all TRACE-P participants for their support. Discussions with C. Potter of NASA Ames, R. Atkinson of UC Riverside, and P. Harley and A. Guenther of NCAR are much appreciated.

References

- Atkinson, R., R. A. Cox, J. Crowley, R. F. Hampson, M. E. Jenkin, J. A. Kerr, M. J. Rossi, and J. Troe, IUPAC evaluated kinetic data, <http://www.iupac-kinetic.ch.cam.ac.uk/>, 2002.
- Andreae, M. O. and P. Merlet, Emissions of trace gases and aerosols from biomass burning, *Global Biogeochem. Cycles*, **15** (4), 955-966, 2001.
- Arlander, D. W., D. Brunking, U. Schmidt, and D. H. Ehhalt, The distribution of acetaldehyde in the lower troposphere during TROPOZ II, *J. of Atm. Chem.*, **22**, 243-249, 1995.
- Arnold, F., et al., Acetone in the upper troposphere and lower stratosphere: Impact on trace gases and aerosols, *Geophys. Res. Lett.*, **24**, 3017-3020, 1997.
- Bey, I et al. Global modeling of tropospheric chemistry with assimilated meteorology: Model description and evaluation, *J. Geophys. Res.*, **106**, 23,073-23,095, 2001.
- Blake, N. J., et al., Influence of southern hemispheric biomass burning on mid-tropospheric distributions of nonmethane hydrocarbons and selected halocarbons over the remote South Pacific, *J. Geophys. Res.*, **104**, 16,213-16,232, 1999.
- Butler, J. H., Better budgets for methyl halides?, *Nature*, **403**, 260-261, 2000.
- Chatfield, R. B.; J. A. Vastano, H. B. Singh, and G. A. Sachse, general model of how fire emissions and chemistry produce African/oceanic plumes (O₃, CO, PAN, smoke) in TRACE A [O₃], *J. Geophys. Res.*, **101**, 24,279-24,306, 1996.
- Crawford, J. et al., Clouds and trace gas distributions during TRACE-P, *J. Geophys. Res.*, in press, 2003.
- Davis, D. D. et al., Trends in western Pacific ozone photochemistry as defined by observations from NASA's PEM-West B (1994) and TRACE-P (2001) field studies, *J. Geophys. Res.*, in press, 2003.
- de Laat, A. T. J., J. A. de Gouw, J. Lelieveld, and A. Hansel, Model analysis of trace gas measurements and pollution impact during INDOEX, *J. Geophys. Res.*, **106**, 28,469-28,480, 2001.
- de Gouw, J. A., C. J. Howard, T. G. Custer, R. Fall, Emissions of volatile organic compounds from cut grass and clover are enhanced during the drying process, *Geophys. Res. Letts.*, **26**, 811-814, 1999.
- Duncan, B. N., R. V. Martin, A. C. Staudt, R. Yevich, and J. A. Logan, Interannual and seasonal variability of biomass burning emissions constrained by satellite observations, *J. Geophys. Res.*, **108**(D2), 4040, doi:10.1029/2002JD002378, 2003.
- Eisele, F. L. et al., Summary of measurement intercomparisons during TRACE-P, *J. Geophys. Res.*, in press, 2003.
- Fall, R., Biogenic emissions of VOCs from higher plants. In: *Reactive Hydrocarbons in the Atmosphere*, C.N. Hewitt (ed.), pp. 43-96, Academic Press, San Diego, 1999.
- Fall, R., Abundant oxygenates in the atmosphere: A biological perspective, Chemical reviews-atmospheric chemistry, in preparation, 2003.
- Fehsenfeld, F. et al., Emissions of volatile organic compounds from vegetation and the implications for atmospheric chemistry, *Global Biogeochem. Cycles*, **6** (4), 389-430, 1992.
- Field, B. D. et al., A global 3-D model evaluation of the methanol budget using TRACE-P observations, *J. Geophys. Res.*, in preparation, 2003.
- Finlayson-Pitts, B. J. and J. N. Pitts, Jr., Chemistry of the upper and lower atmosphere, Academic Press, San Diego, 1999.
- Fried, A., et al., Airborne tunable diode laser measurements of formaldehyde during TRACE-P: Distributions and box-model comparisons, *J. Geophys. Res.*, in press 2003.
- Fuelberg, H. E., C. M. Kiley, J. R. hannon, D. J. Westberg, M. A. Avery, and R. E Newell, Atmospheric transport during the Transport and Chemical Evolution over the Pacific (TRACE-P) experiment, *J. Geophys. Res.*, in press 2003.
- Fukui, Y. and P. V. Doskey, Air-surface exchange of nonmethane organic compounds at a grass land site: Seasonal variations and stressed emissions, *J. Geophys. Res.*, **103**, 13,153-13,168, 1998.
- Galbally, I. E. and W. Kirstine, The production of methanol by flowering plants and the global cycle of methanol, *J. Atmos. Chem.*, **43** (3), 195-229, 2002.

- Goldan, P. D., W. C. Kuster, F. C. Fehsenfeld, and S. A. Montzka, Hydrocarbon measurements in the southeastern United States: The Rural Oxidants in the Southern Environment (ROSE) program 1990, J. Geophys. Res., **100**, 25,945-25,963, 1995.
- Grosjean, D., Formaldehyde and other carbonyls in Los Angeles ambient air, Environ. Sci. & Technol., **16**, 254-262, 1982.
- Guenther, A., et al., A global model of volatile organic compound emissions. J. Geophys. Res., **100**, 8873-8892, 1995.
- Guenther, A. B., et al., Natural emissions of non-methane volatile organic compounds, carbon monoxide and oxides of nitrogen from North America, Atmos. Environ., **34**, 2205-2230, 2000.
- Heald, C. L., et al., Transpacific satellite and aircraft observations of Asian pollution, J. Geophys. Res., submitted, 2003
- Heikes, B. G. et al., Atmospheric methanol budget and ocean implication, Global Biogeochem. Cycles, **16** (4), 80-1 to 80-13, 2002.
- Holzinger, R., C. Warneke, A. Hansel, A. Jordan, W. Lindinger, D. H. Scharffe, G. Schade, P. J. Crutzen, Biomass burning as a source of formaldehyde, acetaldehyde, methanol, acetone, acetonitrile, and hydrogen cyanide, Geophys. Res. Lett., **26**, 1161-1164, 1999.
- Hurst, D. F., D. W. T. Griffith, and G. D. Cook, Trace gas emissions from biomass burning in tropical Australian savannas. J. Geophys. Res., **99**, 16,441-16,456, 1994.
- Iraci, L. T., A. M. Essin, and D. M. Golden, Solubility of methanol in low temperature aqueous sulfuric acid and implications for atmospheric particle composition, J. of Phys. Chem. A, **106** (16), 4054-4060, 2002.
- Isidorov, V. A., I. G. Zenkench, and B. V. Iofe, Volatile organic compounds in the atmosphere of forests, Atmos. Environ., **19**, 1-8, 1985.
- Jacob, D. J., B. Heikes, B., S-M Fan, J. Logan, D. Mauzerall, J. D. Bradshaw, H. B. Singh, G. L. Gregory, and G. Sachse, Origin of Ozone and NO_x in the tropical troposphere: A photochemical analysis of aircraft observations over the south Atlantic basin, J. Geophys. Res., **101**.D19, 24,235-24,250, 1996.
- Jacob, D. J., B. D. Field, E. M. Jin, I. Bey, Q. Li, J. A. Logan, R. M. Yantosca, and H. B. Singh, Atmospheric budget of acetone, J. Geophys. Res., **107**, 5.1-5.19, 10.1029/2001JD000694, 2002.
- Jacob, D. J. et al., The Transport and Chemical Evolution over the Pacific (TRACE-P) mission: Design, Execution and overview of results, J. Geophys. Res., in press 2003.
- Jaeglé, L., D. J. Jacob, W. H. Brune, and P. O. Wennberg, Chemistry of HO_x radicals in the upper troposphere, Atmospheric Environment, **35**, 469-489, 2001.
- Jang, M., N. M. Czoschke, S. Lee, S. and R. M. Kamens, Heterogeneous atmospheric aerosol production by acid-catalyzed particle phase reactions, Science, **298**, 814-817, 2002.
- Jost, C., J. Trentmann, D. Sprung, and A. O. Meinrat, Trace gas chemistry in a young biomass burning plume over Namibia: Observations and model simulations, J. Geophys. Res., in press, 2002.
- Karl, T., A. J. Curtis, T. N. Rosensteil, R. K. Monson, and R. Fall, Transient releases of acetaldehyde from tree leaves- products of a pyruvate overflow mechanism, Plant, Cell and Environ., **25**, 1-11, 2003.
- Karl, T., C. Sprig, J. Rinne, C. Stroud, P. Prevost, J. Greenberg, R. Fall, and A. Guenther, Virtual adjunct eddy covariance measurements of organic compound fluxes from subalpine forest using proton transfer reaction mass spectrometry, Atmos. Chem. and Phys., **2**, 279-291, 2002.
- Kelsey, R. G., Anaerobic induced ethanol synthesis in the stems of greenhouse-grown conifer seedlings, Trees, **10**(3), 183-188, 1996.
- Kesselmeier, J. et al., Emission of short chained organic acids, aldehydes, and monoterpenes from *Quercus ilex* L. and *Pinus pinea* L. in relation to physiological activities, carbon budget, and emission algorithms, Atmos. Environ., **31** (SI), 119-133, 1997.
- Kesselmeier, J. and Staudt, M., Biogenic volatile organic compounds (VOC): An overview on emissions, physiology and ecology, J. of Atmos. Chem., **33**, 23-38, 1999.
- Kimmerer, T. W. and R. C. MacDonald, Acetaldehyde and ethanol biosynthesis in plants, Plant Physiol., **84**, 1204-1209, 1987.
- Kirstine, W., I. Galbally, Y. Ye, and M. Hooper, Emissions of volatile organic compounds (primarily oxygenated species) from pasture, J. Geophys. Res., **103**, 10,605-10,619, 1998.
- Kreuzwieser, J., F. Harren, L. Laarhoven, I. Boamfa, S. Lintel-Hekkert, U. Scheerer, C. Huglin, and H. Rennenberg, Acetaldehyde emissions by the leaves of trees – correlation with physiological and environmental parameters, Physiologia Plantarum, **113** (1), 41-49, 2001.
- Lamanna, M. S., and A. H. Goldstein, In situ measurements of C₂-C₁₀ VOCs above a Sierra-Nevada pine plantation (including oxygenated species) from pasture, J. Geophys. Res., **104**, 21,247 -21,262, 1999.

- Lee, M., Noone, B. C., O'Sullivan, D., and Heikes, B. G. Method for the collection and HPLC analysis of hydrogen peroxide and C₁ and C₂ hydroperoxides in the atmosphere, *J. Atmos. Ocean Technol.*, **12**, 1060-1070, 1995.
- Lee, M., B. G. Heikes, and D. W. O'Sullivan, Hydrogen peroxide and organic hydroperoxide in the troposphere: A review, *Atmos. Environ.*, **34**, 3475-3494, 2000.
- Li, P.; Perreau, K. A.; Covington, E.; Song, C. H.; Carmichael, G. R.; Grassian, V. H., Heterogeneous reactions of VOCs on oxide particles of the most abundant crustal elements: surface reactions of acetaldehyde, acetone and propionaldehyde on SiO₂, Fe₂O₃, TiO₂ and CaO. *J. Geophys. Res.*, **106** (D6), 5517-5529, 2001.
- Lobert, J. M., W. C. Keene, J. A. Logan, and, R. Yevich, Global chlorine emissions from biomass burning: Reactive chlorine emissions inventory, *J. Geophys. Res.*, **104**, 8373-8389, 1999.
- McKeen, S. A., T. Gierczak, J. B. Burkholder, P. O. Wennberg, T. F. Hanisco, E. R. Keim, R.-S. Gao, S. C. Liu, A. R. Ravishankara, D. W. Fahey, The photochemistry of acetone in the upper troposphere: A source of odd-hydrogen radicals, *Geophys. Res. Lett.*, **24**, 3177-3180, 1997
- Martinez, R. D., A. A. Buitrago, N. W. Howell, C. H. Hearn, and J. A. Joens, The near U. V. absorption spectra of several aldehydes and ketones at 300 K, *Atmos. Environ.*, **26A**, 785-792, 1992.
- Mauzerall, D. L., J. A. Logan, D. J. Jacob, B. E. Anderson, D. R. Blake, J. D. Bradshaw, B. Heikes, G. W. Sachse, H. B. Singh, R. Talbot, Photochemistry in biomass burning plumes and implications for tropospheric ozone over the tropical South Atlantic, *J. Geophys. Res.*, **103**(D7), 8401-8423, 1998
- Müller, J.-F., and G. Brasseur, Sources of upper tropospheric HO_x : A three-dimensional study, *J. Geophys. Res.*, **104**, 1705-1715, 1999.
- Nguyen, H. T., N. Takenaka, H. Bandow, Y. Maeda, S. T. de Oliva, M. M. f. Botelho and T. M. Tavares, Atmospheric alcohols and aldehydes concentrations measured in Osaka, Japan and in Sao Paulo, Brazil, *Atmospheric Environment*, **35**, 3075-3083, 2001.
- O'Sullivan, D. W. et al., Long-term and seasonal variations in the levels of hydrogen Peroxide, Methylhydroperoxide, and selected compounds over the Pacific, *J. Geophys. Res.*, in press, 2003.
- Potter, C., S. Klooster, D. Bubenheim, H. B. Singh, and R. Myneni, Modeling terrestrial biogenic sources of oxygenated organic emissions, *Earth Interactions*, in press, 2003.
- Reiner, T., Sprung, D., Jost, C., Gabriel, R., Mayol-Bracero, O. L., Andreae, M. O., Campos, T. L., Shetter, R. E., Chemical characterization of pollution layers over the tropical Indian Ocean: Signatures of emissions from biomass and fossil fuel burning, *J. Geophys. Res.*, **106**, 28,497- 28,510, 2001.
- Riemer, D., et al. Observations of nonmethane hydrocarbons and oxygenated volatile organic compounds at a rural site in the southeastern United States, *J. Geophys. Res.*, **103**, 28,111-28,128, 1998.
- Sander, R, Compilation of Henry's law constants for inorganic and organic species of potential importance in environmental chemistry, <http://www.mpch-mainz.mpg.de/~sander/res/henry.html>, version 3, 1999.
- Sander, S. P., et al., Chemical kinetics and photochemical data for use in stratospheric modeling, Evaluation No. 14, JPL 02-25, <http://jpldataeval.jpl.nasa.gov/>, 2002.
- Schade, G. W., and A. H. Goldstein, Fluxes of oxygenated volatile organic compounds from a ponderosa pine plantation. *J. Geophys. Res.*, **106**, 3111-3123, 2001.
- Schade, G. W., and A. H. Goldstein, Plant physiological influences on the fluxes of oxygenated volatile organic compounds from a ponderosa pine trees. *J. Geophys. Res.*, **107** (D10), 10.1029/2001JD000532, 2002.
- Shepson, P. B., D. Hastie, H. Schiff, M. Polizzi, J. W. Bottenheim, K. Anlauf, G. I. Mackay, and D. R. Karecki, Atmospheric concentrations and temporal variations of C₁-C₃ carbonyl compounds at two rural sites in central Ontario, *Atmos. Environ.*, **25A**, 2001-2015, 1991.
- Sigsby, J.E., S. Tejada, W. Ray, J. M. Lang and J. W. Duncan, Volatile organic compound emissions from 46 in-use passenger cars, *Environ. Sci. and Technol.*, **21**, 466-475, 1987.
- Singh, H. B., "Tropospheric Composition and Analysis: PAN" in *Encyclopedia of Atmospheric Sciences*, J. Holton, J. Pyle, and J. Curry Eds., Academic Press, London, 2002
- Singh, H. B. & Zimmerman, P. B., Atmospheric Distributions and Sources of Nonmethane Hydrocarbons. *Adv. in Env. Sci. and Technol.*, **24**, John Wiley and Sons, New York, 177-235, 1992.
- Singh, H. B. et al., Acetone in the atmosphere: Distribution, sources and sinks, *J. Geophys. Res.*, **99**, 1805-1819, 1994.
- Singh, H. B., M. Kanakidou, P. J. Crutzen, and D. J. Jacob, High concentrations and photochemical fate of oxygenated hydrocarbons in the global troposphere, *Nature*, **378**, 50-54, 1995.
- Singh, H., et al., Distribution and fate of selected oxygenated organic species in the troposphere and lower stratosphere over the Atlantic, *J. Geophys. Res.*, **105**, 3795 –3806, 2000.
- Singh, H. B., Y. Chen, A. Staudt, D. Jacob, D. Blake, B. Heikes, J. Snow. Evidence from the Pacific troposphere for large global sources of oxygenated organic compounds. *Nature*, **410**, 1078-1081, 2001.

- Singh, H. B., A. Tabazadeh, M. J. Evans, B. D. Field, D. J. Jacob, G. Sachse, J. H. Crawford³, R. Shetter, W. H. Brune, Oxygenated volatile organic chemicals in the oceans: inferences and implications based on atmospheric observations and air-sea exchange models, Geophys. Res. Lett., 00, submitted, 2003.
- Staudt, A. C., D. J. Jacob, F. Ravetta, J. A. Logan, D. Bachiochi, T. N. Krishnamurti, S. Sandholm, B. Ridley, H. B. Singh, and B. Talbot, Sources and chemistry of nitrogen oxides over the tropical Pacific, J. Geophys. Res., 108(D2), 8239, doi:10.1029/2002JD002139, 2003.
- Snider, J. R. and G. A. Dawson, Tropospheric light alcohols, carbonyls, and acetonitrile: Concentrations in the southwestern United states and Henry's Law data, J. Geophys. Res., 90(D2), 3797-3805, 1985.
- Solberg, S., C. Dye, N. Schmindbauer, A. Herzog, and R. Gehrig, Carbonyls and nonmethane hydrocarbons at rural European sites from the Mediterranean to the arctic, J. of Atmos. Chem., 25, 33-66, 1996.
- Tabazadeh, A., R. J. Yokelson, H. B. Singh, L. Iraci, and P. Hobbs, Hetrogeneous chemistry on tropospheric clouds involving methanol, in preparation, 2003.
- Tanner, R. L., B. Zielinska, E. Uverna, G. Harshfield, and A. P. McNichol, Concentrations of carbonyl compounds and the carbon isotopy of formaldehyde at a coastal site in Nova Scotia during the NARE summer intensive, J. Geophys. Res., 101, 28,967-28,970, 1996.
- Villanueva-Fierro, I., C. J. Popp, and R. S. Martin, Biogenic emissions and ambient concentrations of hydrocarbons, carbonyl compounds and organic acids from Ponderosa pine and Cottonwood trees of rural and forested sites in central New Mexico, Atmos. Environ., submitted, 2003.
- Warneck, P., Chemistry of the natural atmosphere, second edition, Academic Press, San Diego, 1999.
- Warneke, C., T. Karl, H. Judmaier, A. Hansel, A. Jordan, W. Lindinger, P. J. Crutzen, Acetone, methanol, and other partially oxidized volatile organic emissions from dead plant matter by a biological processes: Significance for atmospheric HO_x chemistry, Global Biogeochem. Cycles, 13, 9-17, 1999.
- Wennberg, P. O., et al., Hydrogen radicals, nitrogen radicals, and the production of ozone in the upper troposphere, Science, 279, 49-53, 1998.
- Wisthaler, A., A. Hansel, R. R. Dickerson, and P. J. Crutzen, Organic trace gas measurements by PTR-MS during INDOEX 1999, J. Geophys. Res., 107 (D19), doi:10.1029/2001JD000576, 2002.
- Yevich, R. and J. A. Logan, An assessment of biofuel use and burning agricultural waste in the developing world, Global Biogeochem. Cycles, in press, 2003.
- Yokelson, R. J., D. E. Ward, R. A. Susott, J. Reardon, and D. W. T. Griffith, Emissions from smoldering combustion of biomass measured by open-path Fourier transform infrared spectroscopy, J. Geophys. Res., 102, 18,865-18,877, 1997.
- Yokelson, R. J. et al., Emissions of formaldehyde, acetic acid, methanol, and other trace gases from biomass fires in North Carolina measured by measured by airborne Fourier transform infrared spectroscopy, J. Geophys. Res., 104, 30,109-30,125, 1999.
- Yokelson, R. J., I. T. Bertschi, T. J. Christian, P. V. Hobbs, D. E. Ward, W. M. Hao, Trace gas measurements in nascent, aged, and cloud-processed smoke from African savanna fires by airborne Fourier transform infrared spectroscopy (AFTIR), J. Geophys. Res., 108(D13), 8485, doi:10.1029/2002JD002352, 2003.
- Zhou, X., and K. Mopper, Carbonyl compounds in the lower marine troposphere over the Caribbean Sea and Bahamas, J. Geophys. Res., 98C, 2385-2392, 1993.
- Zhou, X., and K. Mopper, Photochemical production of low-molecular-weight carbonyl compounds in seawater and surface microlayer and their air-sea exchange, Mar. Chem., 56, 201-213, 1997.

Table 1: Mean concentrations of selected oxygenated organic species and tracers in the Pacific troposphere

Data Selection	Altitude (km)	Acetone (ppt)*	MEK (ppt)	CH ₃ OH (ppt)	C ₂ H ₅ OH (ppt)	CH ₃ CHO (ppt)	C ₂ H ₅ CH O (ppt)	HCHO (ppt)	CH ₃ OOH (ppt)	PAN (ppt)	PPN (ppt)	CO (ppb)	C ₂ Cl ₄ (ppt)
Trop data-no filter	0-2	816±500 (722, 251)	125±145 (81, 251)	1096±1246 (765, 249)	165±246 (75, 197)	371±416 (286, 240)	140±186 (104,251)	469±681 (326, 382)	417±387 (263, 311)	382±566 (165., 301)	30±29 (23, 224)	194 ± 89 (173, 428)	10±9 (9, 393)
	2-4	822±295 (769, 177)	75±52 (64, 177)	1250±691 (1014, 177)	77±69 (47., 139)	226±89 (203, 169)	77±34 (69, 177)	188±133 (165, 264)	364±246 (306, 200)	196±213 (128, 237)	11±13 (7, 174)	151 ± 54 (131, 281)	7±6 (6, 264)
	4-6	725±267 (723, 126)	65±55 (47, 122)	1044±551 (903, 126)	73±70 (45, 87)	173±74 (159, 121)	58±24 (54, 126)	101±69 (88, 175)	265±134 (241, 136)	206±217 (139, 171)	12±14 (7, 109)	131 ± 46 (116, 218)	5±3 (4, 200)
	6-8	685±278 (656, 146)	56±44 (45, 129)	925±533 (852, 146)	56±49 (39, 85)	127±53 (121, 142)	45±18 (43,144)	83±58 (73,186)	190±100 (172,118)	185±146 (156, 195)	9±9 (6, 124)	119± 40 (110, 229)	4±2 (4, 220)
	8-10	660±280 (629, 206)	36±27 (26, 178)	973±681 (815, 206)	61±49 (41, 96)	104±47 (94, 187)	41±17 (38,187)	69±41 (60,238)	194±148 (149,135)	175±158 (123, 266)	7±7 (4, 129)	120 ± 44 (108, 314)	3±2 (3, 294)
	10-12	559±286 (437, 132)	38±25 (31, 81)	777±703 (464, 132)	69±54 (45, 49)	79±45 (64, 123)	33±14 (30, 88)	51±37 (41, 143)	154±89 (130, 76)	111±134 (70, 168)	6±4 (4, 49)	102 ± 36 (86, 206)	2±1 (2, 199)
	0-12	724±358 (669, 1038)	74±90 (54, 938)	1027±839 (818, 1036)	97±151 (48, 653)	199±239 (155, 982)	75±105 (54, 973)	206±401 (110, 1388)	306±278 (220, 976)	222±323 (127, 1338)	15±20 (7, 809)	143 ± 68 (127, 1676)	6±6 (4, 1570)
Trop data-pollution filter**	0-2	466±97 (437, 26)	35± 22 (23, 26)	575± 211 (563, 26)	23± 24 (<20, 26)	204±40 (205, 26)	68± 24 (60, 26)	211± 144 (170, 39)	755± 544 (897, 36)	15± 24 (2, 35)	2 ± 2 (<1, 35)	111± 16 (107, 49)	5± 2 (4, 42)
	2-4	642±207 (636, 80)	48± 33 (42, 80)	840± 258 (744, 80)	33± 41 (23, 80)	173±45 (171, 74)	60± 21 (54, 80)	126± 81 (115, 125)	275± 264 (168, 114)	90± 75 (81, 109)	4 ± 4 (3, 111)	113± 16 (113, 133)	5 ± 2 (5, 123)
	4-6	641±228 (633, 85)	44± 35 (33, 85)	866±406 (812, 85)	31± 28 (24, 85)	148± 48 (145, 80)	53± 21 (51, 85)	89± 60 (76, 119)	208± 155 (204, 112)	117± 86 (102, 117)	4 ± 4 (2, 117)	108± 20 (108, 151)	4± 2 (4, 137)
	6-8	591±239 (573, 106)	37 ± 36 (21, 106)	732 ± 325 (655, 106)	22± 18 (<20,105)	112± 34 (110, 102)	40±15 (38, 106)	79± 60 (67, 143)	125± 111 (110, 129)	130± 75 (132, 148)	4± 4. (2, 147)	102± 17 (104, 177)	3± 2 (3, 167)
	8-10	539± 171 (552, 141)	21± 15 (18, 141)	653± 314 (571, 141)	19± 16 (<20,141)	88± 31 (83, 122)	35± 19 (31, 141)	62± 43 (55, 172)	91± 129 (<25, 157)	108± 78 (98, 179)	1± 2 (<1, 179)	100± 17 (98, 216)	3± 1 (2, 193)
	10-12	444± 203 (389, 98)	15± 17 (<10, 98)	516± 380 (333, 98)	18± 20 (<20, 98)	64± 33 (53, 89)	22± 16 (16, 96)	47± 34 (37, 107)	61± 77 (<25, 109)	64± 69 (35, 130)	1 ± 1 (<1, 130)	86± 18 (8, 160)	2± 1 (2, 151)
	0-12	560± 216 (537, 536)	31± 30 (20, 536)	701± 354 (649, 536)	24± 25 (<20, 535)	117± 56 (110, 493)	42± 23 (41, 534)	87± 76 (67, 705)	181± 253 (105, 657)	99± 80 (88, 718)	3± 3 (<1, 719)	102± 20 (101, 886)	3± 2 (3, 813)

*Mean ± 1 standard deviation (median, number of data points)

** Data are filtered to minimize the effects of pollution (see text)

Table 2: Mean Enhancement Ratios (ER's) and total biomass burning (BB) source estimates of selected Oxidized species

Chemicals (X)	ER/FT-plumes*		ER/MBL-episodes*		Total BB source (Tg y ⁻¹)**	
	$\Delta X/\Delta CO$ (ppt/ppb)	$\Delta X/\Delta CH_3Cl$ (ppt/ppb)	$\Delta X/\Delta CO$ (ppt/ppb)	$\Delta X/\Delta CH_3Cl$ (ppt/ppb)	From FT $\Delta X/\Delta CO$	From FT $\Delta X/\Delta CH_3Cl$
CH ₃ COCH ₃	7.5±1.1	9.0±2.5	4.7±1.9	6.4±2.9	9.3±1.4	9.3±2.6
CH ₃ COC ₂ H ₅	0.7±0.4	0.9±0.7	1.3±0.5	1.6±0.6	2.2±1.2**	2.4±1.8**
CH ₃ OH	16.3±2.0	19.8±6.5	10.6±5.3	16.6±7.5	11.2±1.4	11.3±3.7
C ₂ H ₅ OH	0.9±0.6	1.2±1.1	2.2±1.4	3.7±3.2	1.8±1.2**	2.0±1.8**
CH ₃ CHO	1.4±0.8	1.8±1.3	2.7±2.0	3.9±2.6	--	--
C ₂ H ₅ CHO	0.4±0.3	0.5±0.5	1.4±0.7	1.8±0.8	--	--
PAN	3.8±2.1	4.8±3.4	4.1±1.7	6.6±4.9	--	--
NO _x	0.8±0.7	1.0±0.9	2.1±1.2	3.5±2.8	--	--
HNO ₃	1.3±1.7	1.9±3.2	5.3±1.9	8.5±4.3	--	--
O ₃	260±170	280±170	80±60	130±80	--	--

*Mean ER's with respect to CO and CH₃Cl are based on the sampling of 12 plumes in the free troposphere (FT; 3-10 km) and 9 episodes of marine boundary layer (MBL; 0-1 km) pollution

**The estimated BB source is derived by scaling the FT ERs to a global BB source of 600 Tg y⁻¹/CO and 0.9 Tg y⁻¹/CH₃Cl and is inclusive of primary as well as secondary photochemical sources. MEK and ethanol source estimate correct for loss in transit (see text)

Table 3: Global biomass burning source estimates for selected oxygenated chemicals*

CH ₃ COCH ₃ (Tg y ⁻¹)	CH ₃ OH (Tg y ⁻¹)	MEK (Tg y ⁻¹)	C ₂ H ₅ OH (Tg y ⁻¹)	Type of data	Reference
10 (8-12)**	--	--	--	BB plume at high latitudes	Singh et al. [1994]
7±3	4±2	--	--	Laboratory fires	Holzinger et al. [1999]
--	10±6	--	--	Controlled fires	Yokelson et al. [1999]
5 (3-10)	6 (3-10)	--	--	Assessment	Singh et al. [2000]
3	13	--	--	Assessment	Andreae & Merlet [2001]
5±2	--	--	--	Inverse modeling	Jacob et al. [2002]
21±1**	8±1**	--	--	BB plumes over Indian Ocean	Wisthaler et al. [2002]
9±1**	11±1**	2±1**	2±1**	BB plumes over Pacific	This study (scaled to CO)
9±3**	11±4**	2±2**	2±2**	BB plumes over Pacific	This study (scaled to CH ₃ Cl)

*Most estimates are obtained by scaling measured Enhancement Ratios (ER's) in plumes from biomass combustion to the global CO source

** Inclusive of primary as well as secondary sources attributable to BB emission

Table 4: Global source estimates for selected oxygenated chemicals

Source category	CH ₃ COCH ₃ (Tg y ⁻¹)			CH ₃ OH (Tg y ⁻¹)				MEK	C ₂ H ₅ OH (Tg y ⁻¹)	CH ₃ CHO (Tg y ⁻¹)	C ₂ H ₅ CHO (Tg y ⁻¹)
	Ref. 1	Ref. 2	This study	Ref. 1**	Ref. 3	Ref. 4	Ref. 5	This study	This study	This study	This study
Primary anthropogenic	2 (1-3)	1 (1-2)	2 (1-3)	3 (2-4)	4 (3-5)	8 (5-11)	9	<1	2	<1 (0-1)	<1 (0-1)
Primary biogenic	15 (10-20)	33 (24-42)	50 (25-75)	75 (50-125)	100 (37-212)	280 (50-280)	128	7 ^{##} (5-9)	6 ^{##} (4-8)	35 (20-50)	? (1-5)
Hydrocarbon oxidation*	28 (19-39)	28 (20-36)	28 (20-36)	18 (12-24)	19 (14-24)	30 (18-30)	37	1 (1-3)	2 (1-3)	30 (15-45)	3 (1-5)
Dead/decaying plant matter	6 (4-8)	2 (0-7)	6 (4-8)	20 (10-40)	13 (5-31)	20 (10-40)	23	small	small	small	? (1-5)
Biomass burning	5 (3-10)	4 (3-6)	9 (7-11)	6 (3-17)	13 (6-19)	12 (2-32)	12	2 (1-3)	2 (1-3)	10 (5-15)	? (25-65)
Oceanic	? (37-80)	27 (21-33)	0 (0-15)	? (75-210)	small (83-260)	? (90-490)	0	0 (7-16)	0 (8-17)	125 (75-175)	45 (25-65)
Total source	56 (37-80)	95 (69-126)	95 (57-148)	122 (75-210)	149 (83-260)	345 (90-490)	209	11 (7-16)	12 (8-17)	200 (115-286)	? (115-286)
Estimated source (this study)	95 (τ = 15 d)			110 (τ = 9 d)				11 (τ = 7 d)	12 (τ = 3.5 d)	220 (τ = 1 d)	105 (τ = 1 d)

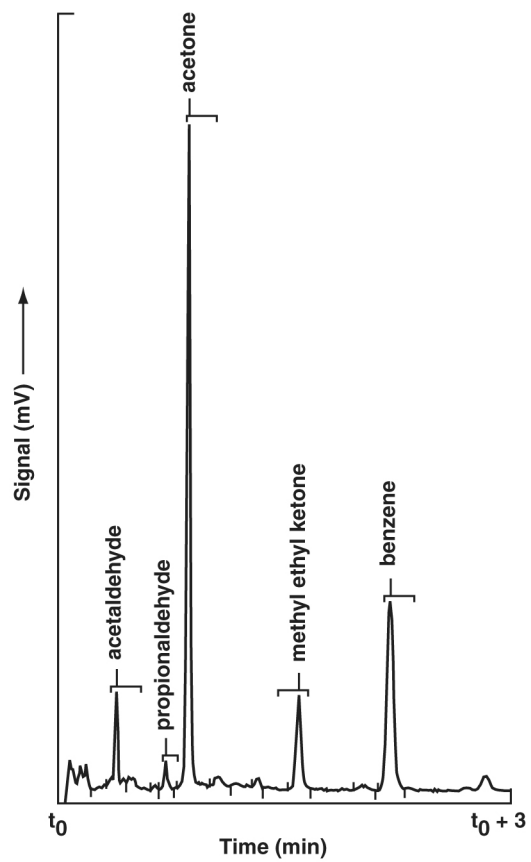
*Main hydrocarbons involved are CH₄ for methanol; C₃H₈, i-alkanes, and terpenes for acetone; n-C₄H₁₀ for MEK, alkanes/alkenes for aldehydes

** Ref. 1-Singh et al. [2000]; Ref. 2-Jacob et al. [2002]; Ref. 3-Galbally et al. [2002]; Ref. 4-Heikes et al. [2002]; 5-Field et al. [2003]

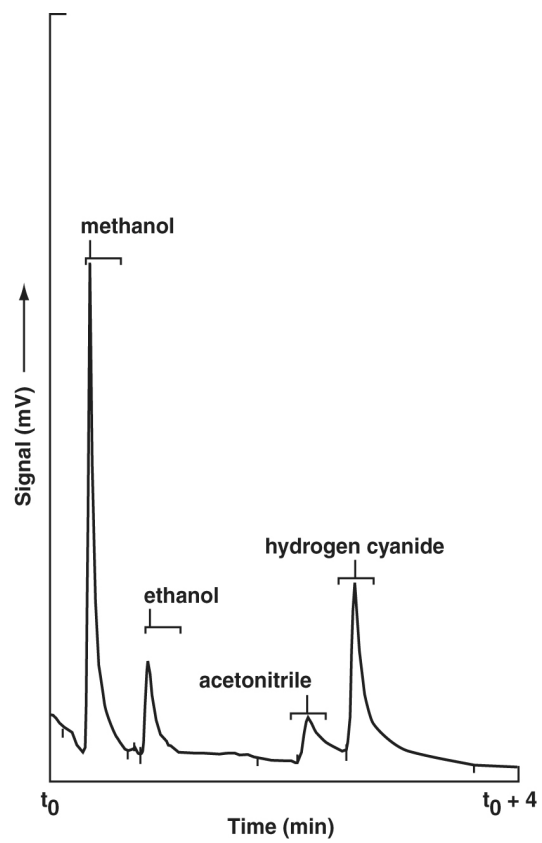
Estimated by normalizing to a 95 Tg y⁻¹ source for acetone (see text)

By difference.

@ Global mean residence time in days



Singh



Singh

Figure 1: A chromatogram showing the separation and detection of oxygenated organic species in ambient air

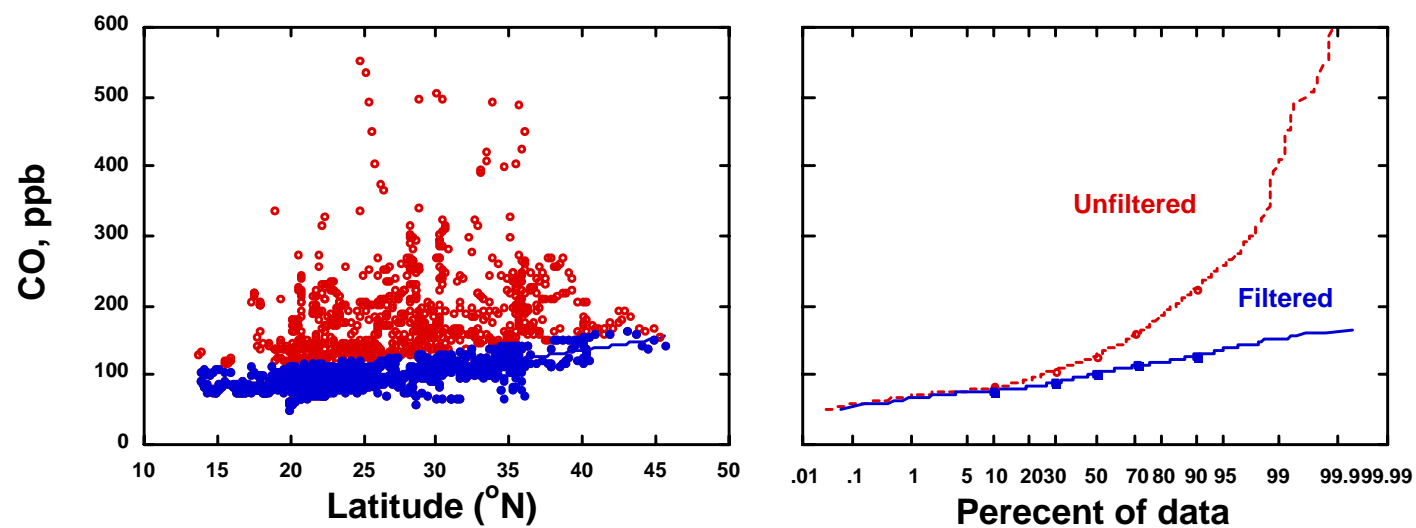


Figure 2: The effect of the “pollution filter” used in this study on CO mixing ratios. The left panel shows the CO data that were excluded (red). The blue data and the line represent the background CO profile assumed in this study. The right panel gives the CO frequency distribution with and without the “pollution filter”.

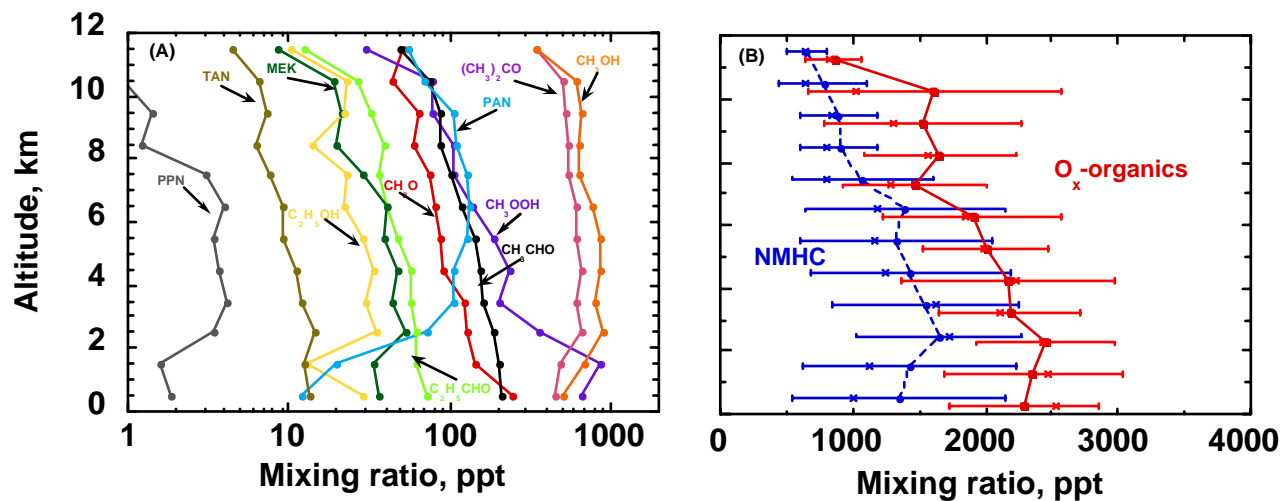


Figure 3: Oxygenated organic chemicals in the Pacific troposphere. (A) Mean altitude profiles of individual oxygenated species; (B) A comparison of total oxygenated volatile organic chemical (Σ OVOC) abundance with that of total non-methane hydrocarbons (Σ NMHC). A variable filter is used to minimize pollution influences (Figure 2). The altitude showing Σ OVOC is shifted by -0.25 km for clarity. TAN is the sum of all alkyl nitrates (Σ RONO₂). See text for more details.

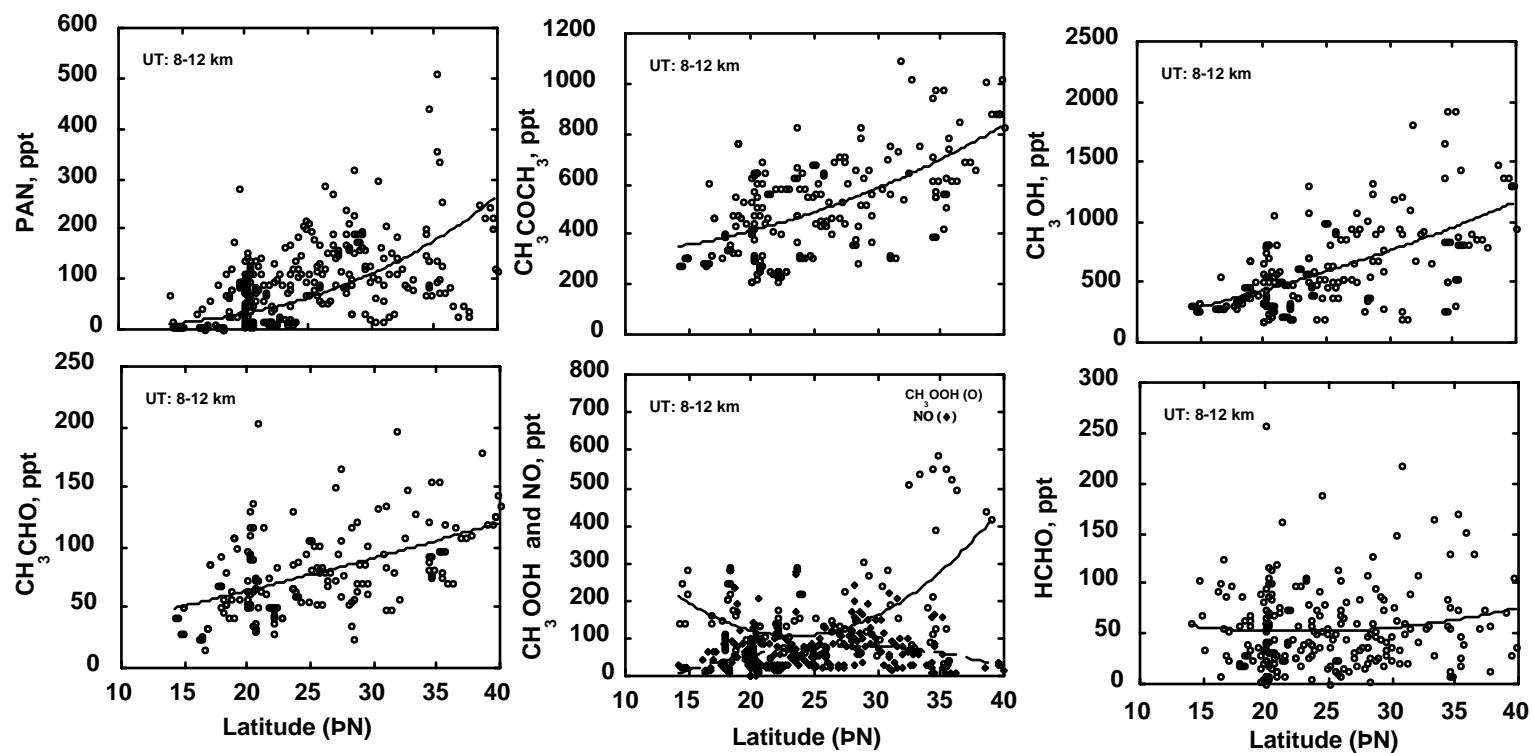


Figure 4: Latitudinal distribution of selected OVOC in the upper troposphere (8-12 km). A filter is used to minimize pollution influences as in Figure 2. The lines represent a best fit to the data.

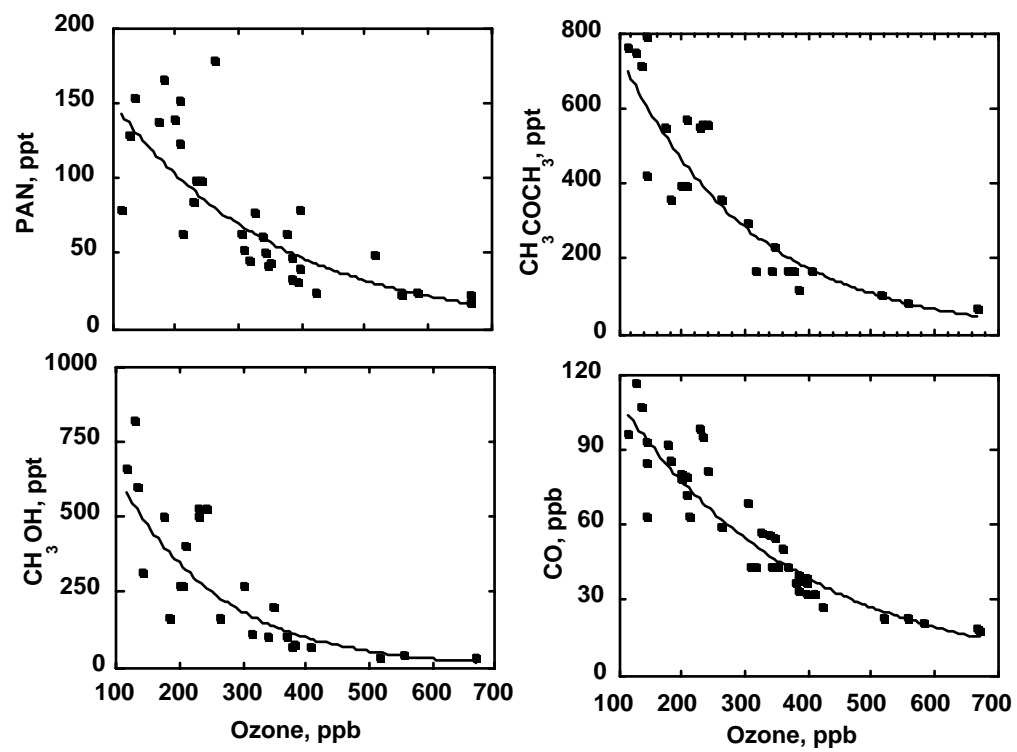


Figure 5: Distribution of selected OVOC and CO in the lowermost stratosphere.

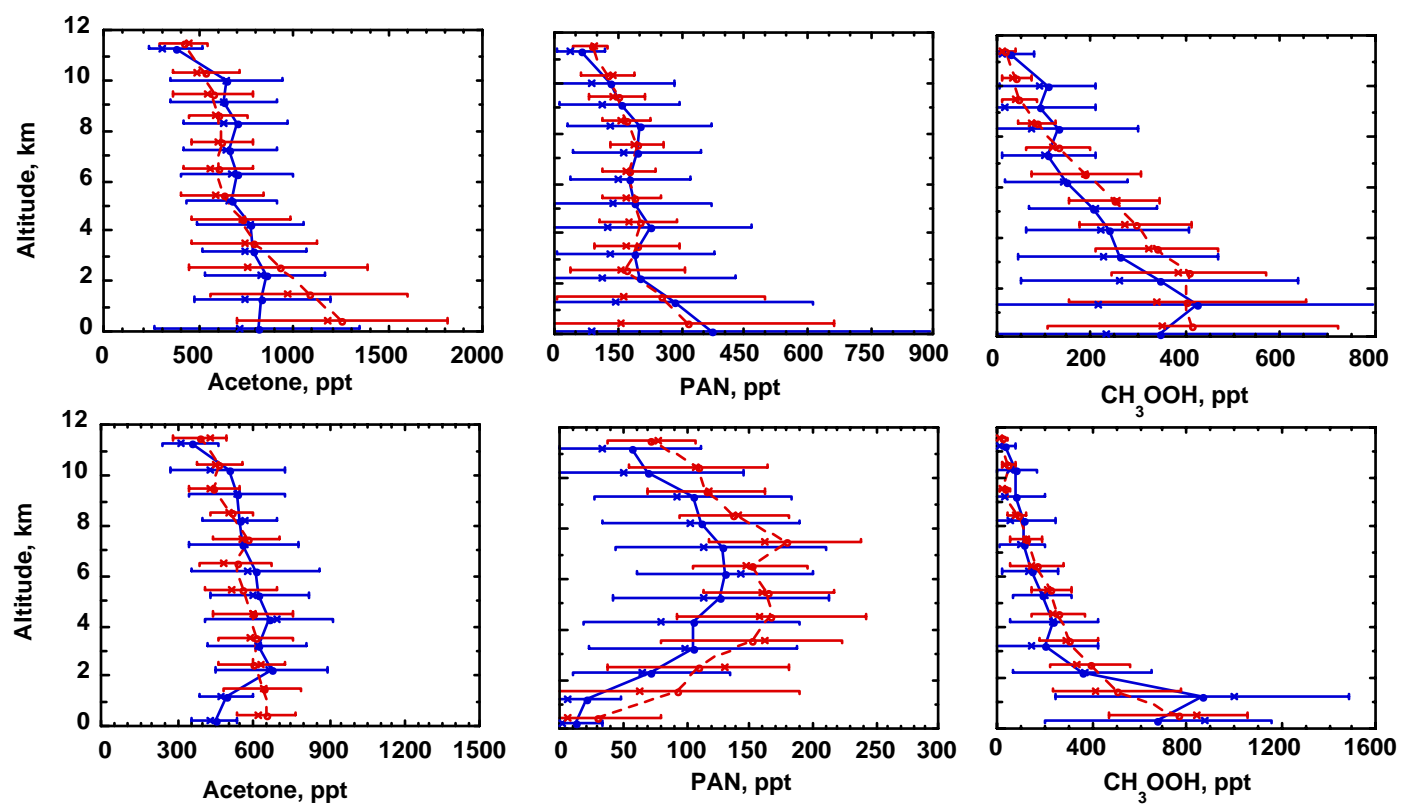


Figure 6: A comparison of the measured (solid line) and GEOS-CHEM modeled (dashed line) distribution of selected OVOC. Top panels represent all data in the troposphere. Bottom panels are data filtered to minimize pollution influences as in Figure 2.

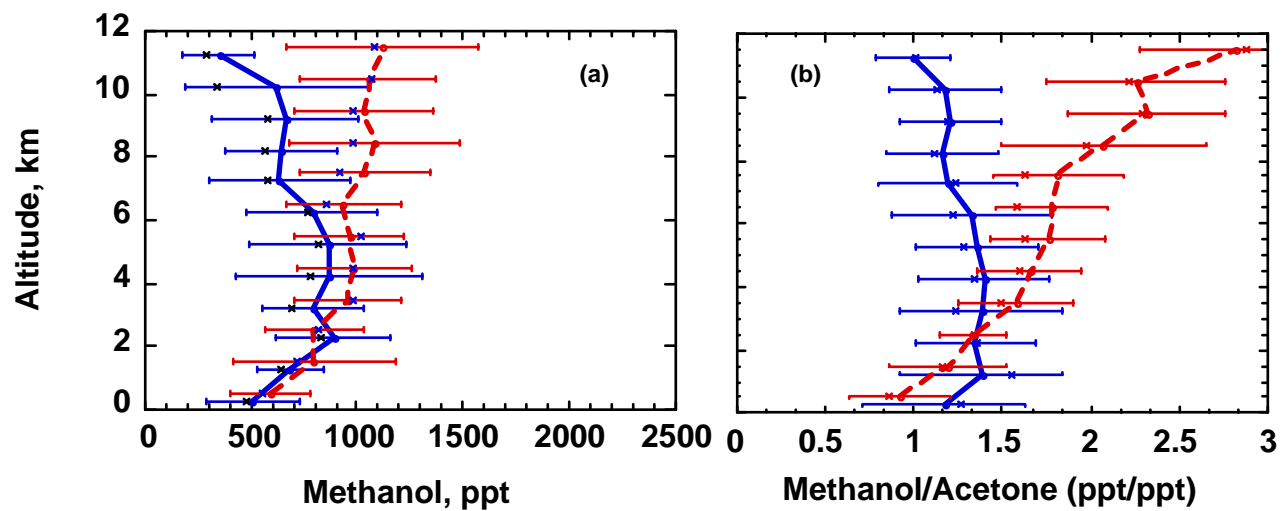


Figure 7: A comparison of observed and modeled methanol and methanol to acetone ratio. Filtered data as in Figure 2.

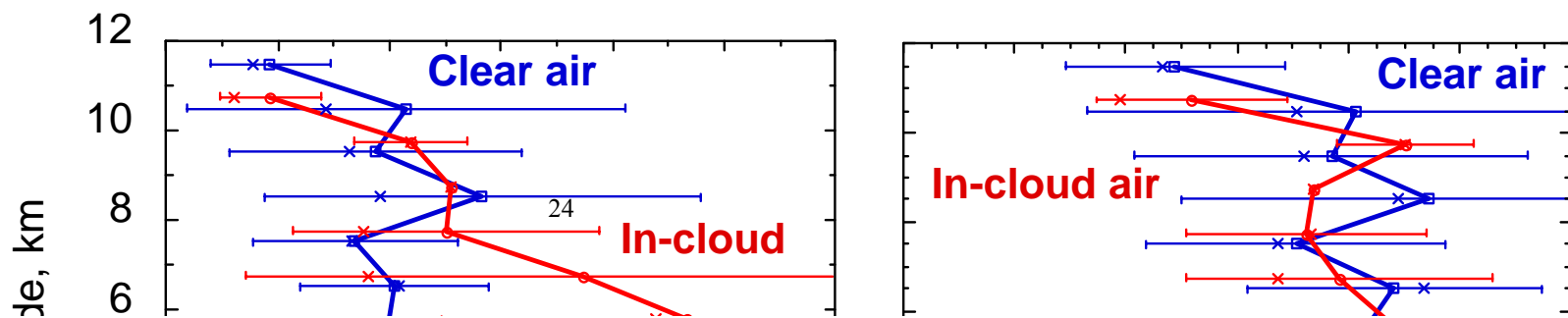


Figure 8: Methanol and methanol/CO in cloudy and clear air during TRACE-P. Clear air data shifted by -0.25 km for clarity.

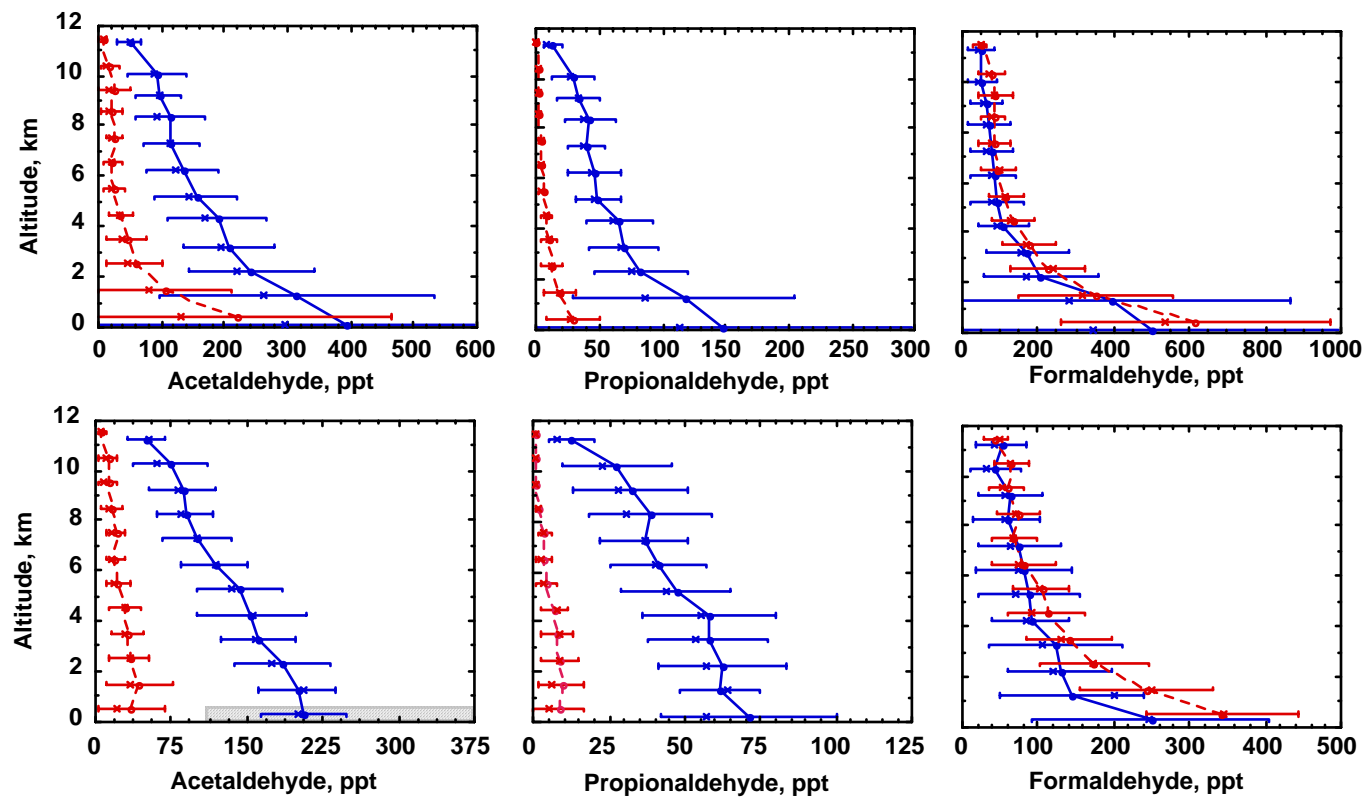


Figure 9: A comparison of the measured (solid line) and modeled (dashed line) distribution of aldehydes. Shaded area in the bottom left shows range of other measurements. As in figure 6.

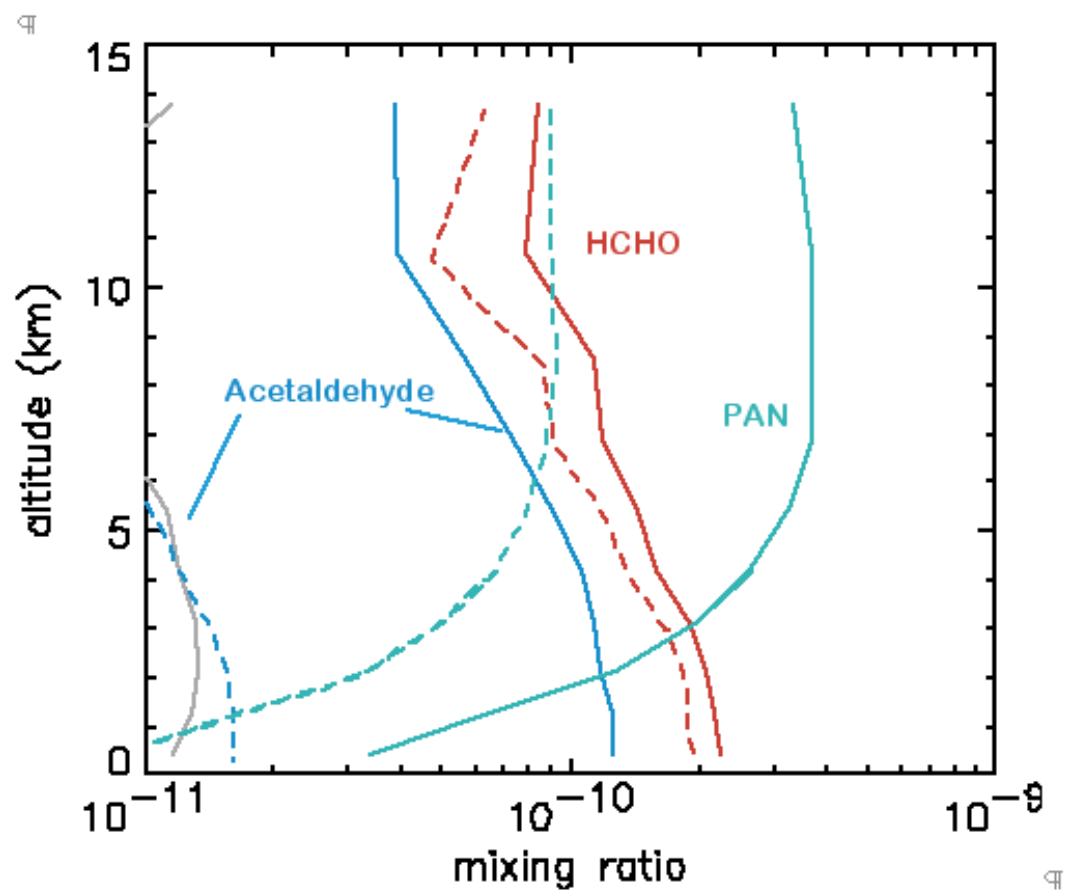


Figure 10: A 1-D model simulation of the potential contribution of observed acetaldehyde concentrations to formaldehyde and PAN formation.

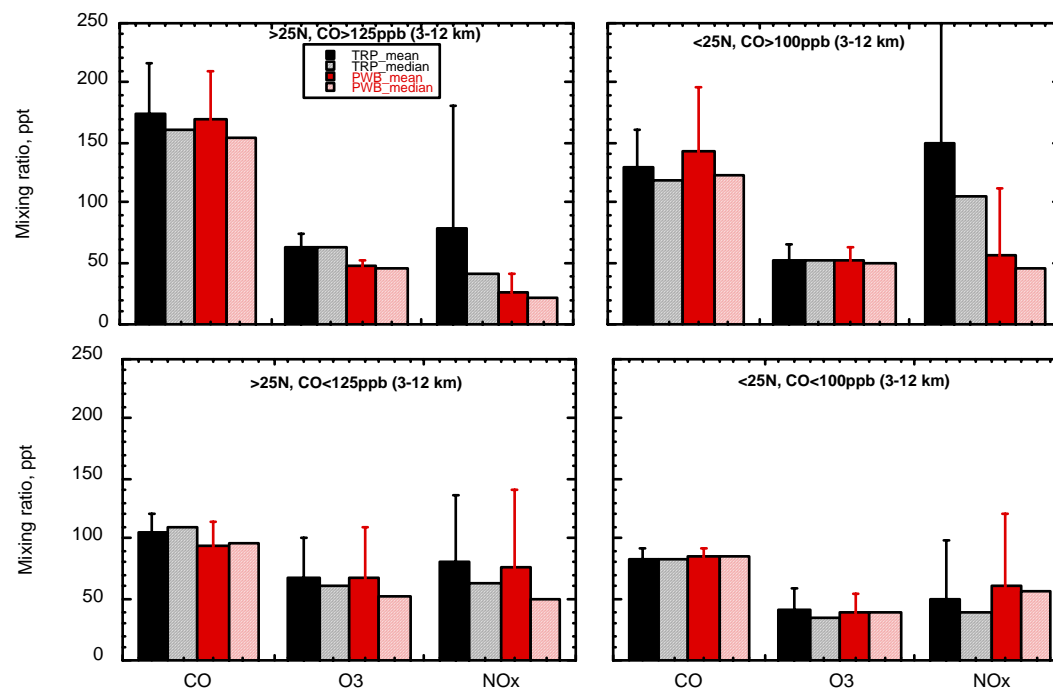


Figure 11: A comparison of TRACe-P (black) and PEM-West B (red) mixing ratios of CO, O₃ and NO_x at mid- and subtropical latitudes under pristine and polluted conditions. Solid colors represent means; dashed lines are medians.

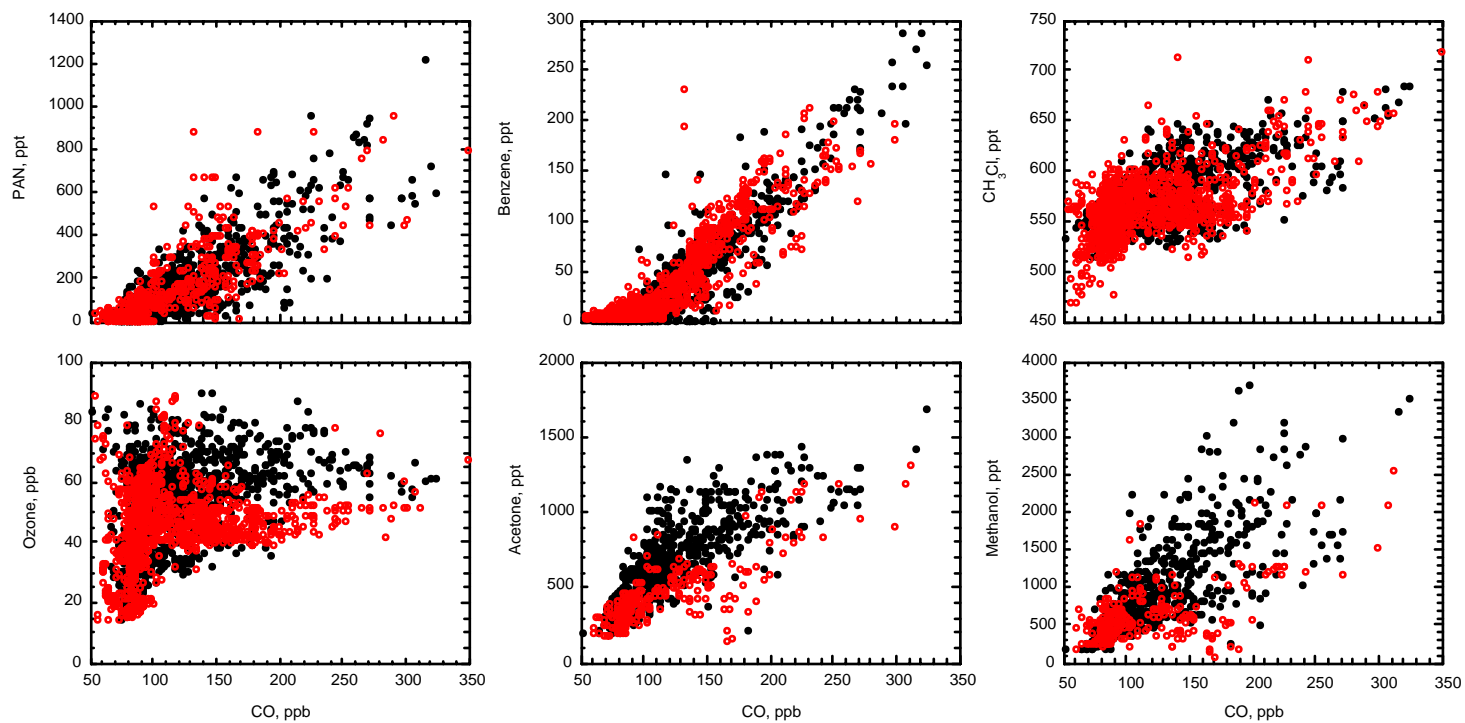


Figure 12: A comparison of data collected in the free troposphere (3-12 km) during PEM-West B (red) and TRACE-P (black) normalized against CO.

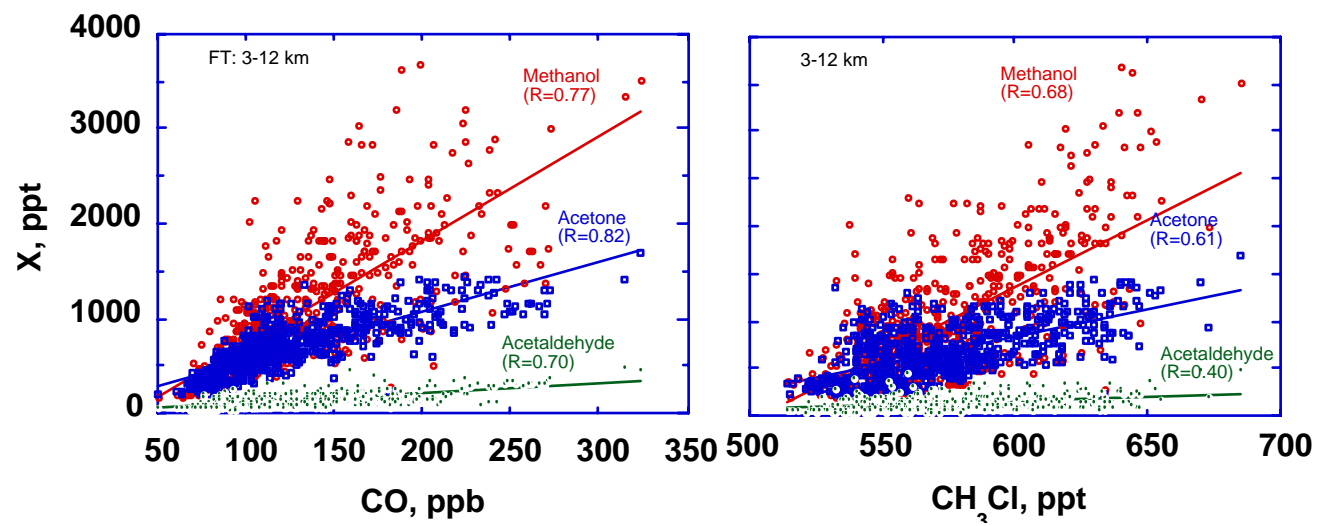


Figure 13: Relationships between selected OVOC and tracers in the free troposphere

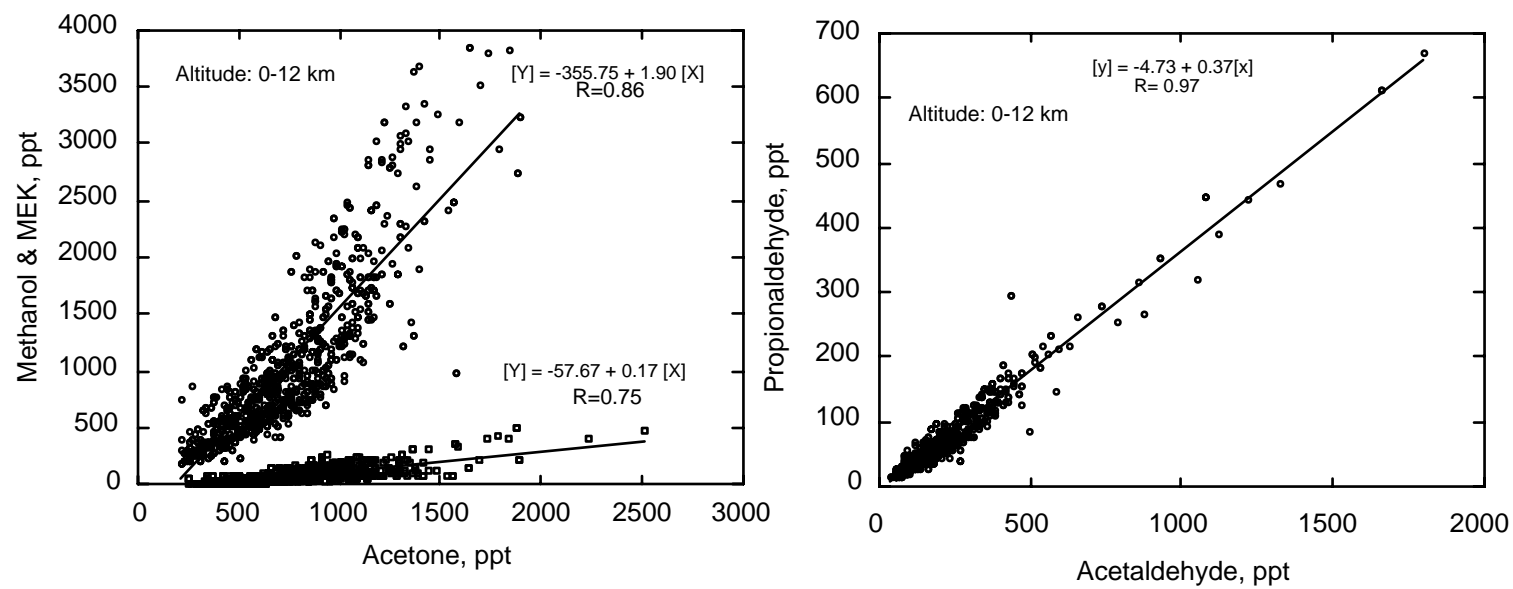


Figure 14: Relationships among carbonyls and alcohols in the Pacific troposphere